



Pacific Northwest
NATIONAL LABORATORY

Proudly Operated by Battelle Since 1965

Affordable Hybrid Heat Pump Clothes Dryer

June 2016

W TeGrotenhuis
A Butterfield

D Caldwell
A Crook

DISCLAIMER

This report was prepared as an account of work sponsored by an agency of the United States Government. Neither the United States Government nor any agency thereof, nor Battelle Memorial Institute, nor any of their employees, makes **any warranty, express or implied, or assumes any legal liability or responsibility for the accuracy, completeness, or usefulness of any information, apparatus, product, or process disclosed, or represents that its use would not infringe privately owned rights.** Reference herein to any specific commercial product, process, or service by trade name, trademark, manufacturer, or otherwise does not necessarily constitute or imply its endorsement, recommendation, or favoring by the United States Government or any agency thereof, or Battelle Memorial Institute. The views and opinions of authors expressed herein do not necessarily state or reflect those of the United States Government or any agency thereof.

PACIFIC NORTHWEST NATIONAL LABORATORY

operated by

BATTELLE

for the

UNITED STATES DEPARTMENT OF ENERGY

under Contract DE-AC05-76RL01830

Printed in the United States of America

Available to DOE and DOE contractors from the
Office of Scientific and Technical Information,
P.O. Box 62, Oak Ridge, TN 37831-0062;
ph: (865) 576-8401
fax: (865) 576-5728
email: reports@adonis.osti.gov

Available to the public from the National Technical Information Service
5301 Shawnee Rd., Alexandria, VA 22312
ph: (800) 553-NTIS (6847)
email: orders@ntis.gov <<http://www.ntis.gov/about/form.aspx>>
Online ordering: <http://www.ntis.gov>



This document was printed on recycled paper.

(8/2010)

Affordable Hybrid Heat Pump Clothes Dryer

W TeGrotenhuis, Ph.D.¹ D Caldwell¹
A Butterfield² A Crook²

June 2016

Prepared for
the U.S. Department of Energy
under Contract DE-AC05-76RL01830

Pacific Northwest National Laboratory
Richland, Washington 99352

¹ Pacific Northwest National Laboratory

² Jabil

Executive Summary

This project was successful in demonstrating the feasibility of a step change in residential clothes dryer energy efficiency by demonstrating heat pump technology capable of 50% energy savings over conventional standard-size electric dryers with comparable drying times. A prototype system was designed from off-the-shelf components that can meet the project's efficiency goals and are affordable. An experimental prototype system was built based on the design that reached 50% energy savings. Drying times with the prototype were over 60 minutes compared to the target of 40 minutes, but improvements have been identified that will reduce drying times and further increase energy savings. The energy efficiency of the prototype was 30% higher than heat pump dryers recently introduced to the U.S. market with comparable drying times of around 60 minutes, representing a step change in the technology.

Two innovations have been implemented that enable higher energy efficiency. Heat pumps reduce the power used by a dryer by recycling heat from the moist drum exhaust air to the incoming dry air. However, heat pumps are slower in the initial warm-up phase, and it is difficult with available heat pump technology to heat the incoming air as hot as an electric element, resulting in much longer drying times. The 'hybrid' solution demonstrated in the current project adds an electric heater in combination with a heat pump. This creates a trade-off between energy efficiency and drying time depending on how much the heater is used. Another significant innovation is incorporating a recuperative heat exchanger to facilitate heat transfer directly from the exhaust to the inlet air with very little energy input, which offsets the power required by both the heat pump and the electric element. The recuperator is particularly effective at saving energy at the end of the cycle when the load is mostly dry by allowing the heater and heat pump to be turned off earlier. The final innovation is a novel design of the heat pump condenser using standard tube-fin heat exchanger technology. This design increases the heating by the heat pump and lowers the power to the low-efficiency electric element.

The current prototype was built by modifying a commercial standard vented electric clothes dryer with known energy efficiency from previous testing [1]. A model of the electric dryer was validated using test data and then modified to incorporate a heat pump and recuperator. Modeling facilitated design of a hybrid heat pump clothes dryer and predicted 50% lower energy use at the same drying time of 40 minutes. A demonstration system was built from the design that involved constructing a heat pump system, modifying the standard commercial dryer, and integrating them into a demonstration system. The system was tested under controlled ambient conditions in an environmental chamber following the protocols of the standard DOE D2 Test Procedure [2]. Two types of tests were performed. The 'NORMAL' tests used the electric element through most of the cycle in favor of shorter drying times, and the 'ECO' tests only used the element at the start in the warm-up phase in favor of energy efficiency. In ECO mode, energy savings of over 50% compared to the unmodified standard electric dryer were achieved in drying times of over an hour. These results also represent 30% savings compared to heat pump dryers recently introduced to the U.S. market. Energy savings in NORMAL mode were typically in the range of 40–45% with drying times under an hour.

Discrepancies between design and measured performance of the prototype represent opportunities for improving the prototype. Analyses of the test data revealed the likelihood of air leaking into the drum, most likely from around the door, as well as air bypassing the drum. These leaks can be easily rectified. A bigger issue is the pressure drop of the recuperative heat exchanger, which accounted for 84% of the increased pressure drop. Reducing pressure drop is the most substantive opportunity to improve on the prototype system. Possible solutions include developing alternative technology to the stacked-plate heat exchanger that was used.

The issue of affordability was addressed through a simple payback analyses. A bottoms-up analysis based on quoted costs of components at volume indicates a payback of less than 9 years for 25% of the U.S. residential market. It is expected this could be reduced to less than 5 years with additional supply chain negotiations and further refinements of the design and components. An energy savings of 50% would provide justification of incentive programs by utilities. Already, New Jersey is offering an incentive of \$300 for the Blomberg compact vent-less dryer, and Puget Sound Energy is offering \$150 for heat pump dryers.

Overall, substantial progress was in showing the potential for significantly higher energy efficiency in standard residential clothes dryers utilizing novel heat pump clothes dryer technology. A next step is to develop a true prototype that eliminates the shortcuts that were taken, packages the heat pump system into a pedestal under the dryer, and resolves the issues identified above. Additional development of the control system is needed to optimize energy savings and to add auto termination. These future developments are intended to be accomplished with the help of OEM expertise. With these improvements the technology demonstrated here could be ready for market in the near term.

Acknowledgements

This work was sponsored by the Bonneville Power Administration (BPA) through the Technology Innovation program. Robert Weber served as the BPA Project Manager. Ward TeGrotenhuis served as the PNNL Project Manager, with help from Graham Parker, who was the co-Project Manager focused on outreach to utilities and energy efficiency communities.

Many thanks are extended to others who assisted with the modeling, assembly, and testing of the Hybrid Heat Pump Clothes Dryer demonstration system. Alex Crook at Jabil led the assembly of the heat pump system and performed the payback analysis. Dustin Caldwell completed the CAD design of the demonstration system, and assisted with assembly, start-up, and trouble-shooting. Austin Winkelman assisted with modeling and assembly of the demonstration system. Ben Roberts developed the data acquisition and control system and assisted with assembly and start-up of the demonstration system. Rick Pratt provided electrical support, including designing and implementing the dryer controls and power metering, and assisted with start-up and trouble-shooting. Tim Veldman assisted with assembly. Kevin Gervais performed testing of the demonstration system.

Contents

Executive Summary	iii
Acknowledgements.....	v
1.0 Introduction	1.4
1.1 Overview	1.4
1.2 Background	1.6
1.3 Technical Approach	1.8
2.0 Hybrid Heat Pump Clothes Dryer Design	2.1
2.1 Conventional Electric Clothes Dryer Model	2.1
2.2 Drying Cycle Simulation of an Electric Dryer	2.5
2.3 Hybrid Heat Pump Clothes Dryer Model.....	2.7
2.4 Hybrid Heat Pump Clothes Dryer Design.....	2.9
3.0 Demonstration of Hybrid Heat Pump Clothes Dryer.....	3.1
3.1 Components and Assembly	3.1
3.2 Data Acquisition and Control and Test Procedure	3.5
3.3 Test Results	3.7
3.4 Evaluation of Demonstrator Performance	3.14
4.0 Payback Analysis.....	4.1
5.0 Conclusions and Recommendations	5.1
6.0 References	6.1
Appendix A.....	A.1

Figures

1.1. Schematic of the HyHPCD	1.5
1.2. Example of warm-up, bulk dry, and high heat stages of an automatic termination cycle from testing of Test Unit 1 with the AHAM 1992 load on COTTONS and high temperature settings; the power profile on the right shows when one or both heating elements are on along with the RMC data obtained from the scale measurements.	1.10
2.1. ChemCAD flowsheet of a conventional electric dryer	2.1
2.2. Quadratic fit of drying rate to RMC during the FRDP phase of a drying cycle	2.4
2.3. Fit of drying rate to $(T_{\text{exhaust}} - T_{\text{ambient}})$ during the warm-up phase of a drying cycle	2.5
2.4. Comparison of exhaust RH and temperatures between the ChemCAD simulation (CC) and the experimental measurements	2.6
2.5. Comparison of RMC between the electric dryer model (CC) to the experimental measurements of the AHAM 2009 test.....	2.7
2.6. ChemCAD flowsheet of a hybrid heat pump clothes dryer	2.8
2.7. Comparison of exhaust temperatures between the original electric dryer data, the electric dryer model results, and the HyHPCD model results, including both drum exhaust and evaporator exhaust for the HyHPCD.	2.11
2.8. Comparison of RMC profiles between the original electric dryer data, the electric dryer model results, and the HyHPCD model results	2.11
2.9. Energy profile of the HyHPCD model results, including power inputs to the compressor and element, overlaid on a stacked-chart of the heating of the incoming air by the recuperator, the heat pump, and the electric element.	2.12
2.10. Efficiency of heating the drying air during the drying cycle of a HyHPCD.....	2.13
3.1. GE Model GTDN550ED standard vented electric dryer that was instrumented, placed on a scale for measuring RMC, and tested following the DOE Test Procedures in a previous PNNL project [1].	3.1
3.2. CAD drawing of the GE Model GTDN550ED standard vented electric dryer on top of the heat pump system.....	3.3
3.3. Heat pump CAD design	3.3
3.4. Dryer cabinet with drum removed showing added baffling and insulation and the internal duct from the blower.....	3.4
3.5. The heat pump subsystem during the assembly process; heat exchangers with interconnecting plenums on the left and the refrigerant loop on the right	3.4
3.6. The HyHPCD system next to the environmental chamber used for testing.....	3.5
3.7. Comparison of results with the DOE test load to the original electric dryer, the 50% savings target, and commercial standard-size heat pump dryer; data are divided between higher and lower final RMC for the ECO and EXPRESS modes	3.9
3.8. Temperatures of the drying air through the cycle for Test 10.....	3.10
3.9. Relative humidity of the drying air through the cycle for Test 10.....	3.11
3.10. Power consumption of the compressor and combined heaters and drum motor through the cycle for Test 10	3.11

3.11. Effects of heat power and final RMC of the load on EF for the two test modes, ECO and EXPRESS, and two test loads, the standard DOE and AHAM 1992 loads.....	3.13
3.12. Refrigerant piping temperatures through the cycle for Test 10	3.14
3.13. Calculated ratio of cold stream to hot stream heat duties in the recuperator assuming equal air flow on both sides.....	3.15
A.1. Front and side views of the condenser component designed and made to specifications by Super Radiator Coils; coffee cup is included for perspective.	A.1
A.2. Front view of the evaporator component designed and made to specifications by Super Radiator Coils.	A.2
A.3. Two recuperative heat exchangers of different size obtained from HeatEx; the smaller heat exchanger was used in the heat pump system.....	A.2
A.4. Embraco Model FFI12HBX-EJ compressor shown being installed in the heat pump system.....	A.3
A.5. Final specifications for the condenser component from Super Radiator Coils.	A.4
A.6. Final specifications for the subcooler component from Super Radiator Coils.....	A.5
A.7. Final specifications for the evaporator component from Super Radiator Coils.	A.6
A.8. Final specifications for the recuperator component from HeatEx.	A.7
A.9. Drawing of the Condenser Coil from Super Radiator Coils.	A.9
A.10. Drawing of the Evaporator Coil from Super Radiator Coils.....	A.10

Tables

1.1. Heat pump clothes dryers in the U.S. residential market.....	1.7
1.2. Heat pump clothes dryer energy savings and simple payback when compared to similar ENERGY STAR electric (only) models	1.7
3.1. Tests performed with the HyHPCD demonstration system indicating test load used, nominal heater power, when the heaters and heat pump compressor were turned off, and drum exhaust temperatures.....	3.8
3.2. Test results including the load RMC at the end of the test, calculated EF, energy savings relative to the baseline dryer and the DOE ECS, and the drying time.....	3.9
3.3. Energy breakdown for the HyHPCD tests including average measured heater and compressor power, total energy consumed, and breakdown of energy use between heaters, compressor, and motor, as well as cool-down period at the end-of-cycle with only drum motor running	3.12
3.4. Design pressure drops for the heat pump heat exchangers	3.17
4.1. Energy cost savings and payback based on upper and lower projections of \$530 and \$210 price increases for a HyHPCD over conventional standard electric dryers for the top 25% heaviest users in the U.S. market.....	4.2
4.2. Rebates for meeting a 5-year payback for 25% of consumers based on the upper bound marginal price of \$530 for a HyHPCD	4.2
4.3. Major component costs based vendor quotes for the HyHPCD.....	4.3
A.1. Correlation coefficients for the Embraco Model FFI12HBX-EJ compressor where ET and CT are the evaporation and condensation temperatures, respectively.	A.8

1.0 Introduction

1.1 Overview

With funding support from the Bonneville Power Administration (BPA) Technology Innovation program, Pacific Northwest National Laboratory (PNNL) in partnership with Jabil, a US-based global manufacturing services provider, has designed, constructed, and demonstrated feasibility of a hybrid heat pump clothes dryer (HyHPCD) suitable for the U.S. Market. The primary objective was to demonstrate that energy savings of at least 50% over conventional electric dryers is achievable with a payback of less than 5 years for at least 25% of the Bonneville Power Administration (BPA) residential customers.

The primary metric for energy efficiency of clothes dryer is the energy factor (EF) in units of lbs/kWh, defined as the ratio of the mass of the dry load to the total energy consumed by the drying cycle. DOE has established standard test procedures for measuring energy factors that specify all the details necessary for performing a valid measurement of EF, including size and composition of the load, ambient temperature and humidity, and how to operate the dryer [2]. The test procedures also account for stand-by and off-mode energy consumption in a combined energy factor (CEF). Typically, the energy use in these modes is incidental, and in this report, comparisons are made between CEF and EF, which includes only the energy used during the drying cycle. DOE has two published test procedures. The D1 procedure dictates a timed-dry test and requires the cycle to be manually stopped when the final residual moisture content (RMC) of the load reaches between 2.5% and 5% [3]. The optional D2 procedure requires a dryer with automatic termination to be operated to end-of-cycle and requires the final RMC to be below 2%. The new 2015 energy conservation standard (ECS) requires a CEF of greater than 3.73 lbs/kWh for standard vented electric dryers using either the D1 procedure or the optional D2 Test Procedure.

The novel HyHPCD concept overcomes two primary hurdles of introducing a high efficiency heat pump dryer to the U.S. residential market—higher purchase cost and long drying times. This is accomplished by using a hybrid combination of a heat pump and an electric element to heat the air entering the drum, as shown in Figure 1.1. Air drawn in from the room is heated before entering the drum in a sequence of three steps. First, heat is recovered from the hot, moist air coming from the drum in a recuperative heat exchanger. Next, heat is added from the condenser of the heat pump. Finally, an electric element heats the air last before it enters the drum. The hot, moist exhaust from the drum is first cooled by the heat exchanger and then by the evaporator of the heat pump before being vented. The objective is to heat the air to a temperature that is comparable to conventional electric dryers so that the drying time is not longer. Off-the-shelf heat pump technology, typically used in refrigerators and air conditioners, cannot currently heat the air as hot as an electric element in a conventional dryer, so without an electric element as the last step, the air will not enter the drum as hot, resulting in longer drying times.

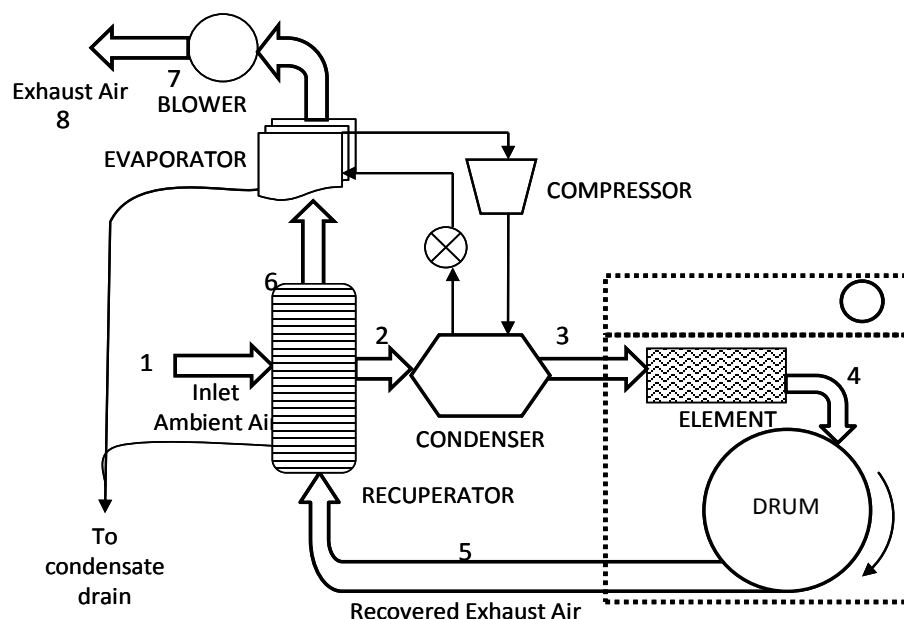


Figure 1.1. Schematic of the HyHPCD. Large arrows indicate air flow, and thin arrows indicate heat pump circuit or condensate flow.

From the perspective of energy cost in terms of power consumed per unit of heat added to the drying air, the recuperator is the cheapest but lowest temperature source. The only ‘cost’ is the additional blower power to overcome the added pressure drop, but the quantity and temperature are limited by the drum exhaust temperature. The electric element has the highest energy cost because the heat added is equal to the power consumed, although higher temperatures can be reached. The heat pump efficiency determines the ratio between heating and power consumption, which consists of the compressor power and increased blower power to move the air through the condenser and evaporator. Heat pump efficiency decreases with increasing condenser temperature, so the energy cost—the ratio of power consumption to heat added—of the heat pump varies with operating conditions. The goal is to use the cheapest combination of heat sources throughout the cycle in order to use as little power as possible with the constraint of a reasonable drying time. Therefore, the recuperative heat exchanger is always used while the electric element is used as little as necessary. Understanding the drying process is essential for optimizing the design and operation of the HyHPCD. The next section provides details of the drying process, which is applied subsequently in designing the HyHPCD.

Adding a heat pump to a conventional electric (or gas) dryer will increase purchase cost. The hybrid concept can minimize the increase because of the ability to downsize the expensive heat pump components, which would only need to provide half of the energy needed to heat the drying air to normal operating temperature. In addition to being less expensive, normal drying times are possible because the element is able to heat the air to normal operating temperatures, thereby overcoming the second hurdle, excessive drying time, necessary for penetrating the U.S. market. A payback analysis that incorporates these advantages is provided in Section 4.0.

The HyHPCD offers other advantages over heat pump dryers that are currently on the market. The electric element gives operating flexibility that enables a range of dryer settings, such as ‘ECO-DRY’, that reduces power to the electric element. This allows the consumer to choose higher efficiency and lower operating temperature with the trade-off of longer drying time. A setting that is gentler on the clothes with the potential to reduce wear while also increasing efficiency is a marketable feature that can justify higher purchase cost to consumers. Meanwhile, a ‘NORMAL’ setting gives consumers the

performance they have come to expect from conventional dryers at 50% energy savings. Furthermore, the electric element provides a mechanism for demand-response for grid stability and reducing peak demand, which would be more difficult with conventional ventless HP dryer technologies. Converting from the ventless configuration of existing HPCD products to a vented configuration, as shown in Figure 1.1, enables another opportunity for energy savings. The exhaust air has lower moisture content than conventional electric dryers because the majority of the water is condensed, which makes it more suitable for exhausting into the laundry room or space during the winter. This saves HVAC energy that is normally expended when air is drawn from outside to replace the air that is vented by the dryer. Another advantage of venting the air is to eliminate the potential of lint fouling in half of the air pathway, including the cold side of the air-to-air heat exchanger, the condenser, and the heating element. Lint accumulation on the electric element is a fire hazard that is avoided by venting the air. Others have managed lint fouling by incorporating a disposable filter or increasing the fin pitch of heat exchangers. In the proposed hybrid HPCD, access will be provided for removing and cleaning the air-to-air heat exchanger. Lint fouling of the evaporator will be minimized by using a higher fin pitch than the recuperative heat exchanger. The combination of existing lint mitigation approaches and design flexibility offers multiple solutions to managing lint fouling.

1.2 Background

In 2010, nine manufacturers were producing 25 models of heat pump dryers only for the European and Asian markets [4]. However, these units are not appropriate for the North American mass market for many reasons. These heat pump clothes dryers are dimensionally smaller (~23 inches wide) and operate at a lower temperature that typically doubles the drying time compared to conventional standard (27 inch) dryers. Prices for heat pump dryers in Europe ranged from 800 Euros to over 2500 Euros, resulting in long payback periods in the U.S. due to the higher cost [5]. Therefore, a heat pump clothes dryer designed specifically for the U.S. market is required to overcome these issues and obtain the significant energy savings that are possible in U.S. residential energy use. This need has been recognized by the Super Efficient Dryer Initiative and is supported by their sponsors and stakeholders, including the Collaborative Labeling and Appliance Standards Program (CLASP), the Northwest Energy Efficiency Alliance (NEEA), multiple electric utilities, and the Consortium for Energy Efficiency (CEE).

The first heat pump clothes dryers were introduced into the U.S. market over the past couple of years. Table 1.1 shows the brand and model number for four dryers—three standard-size dryers and one compact model. Two of the three standard dryers are vented while the third is unvented. CEF and drying times were obtained from the EPA ENERGY STAR website¹. Energy savings are calculated relative to the DOE Energy Conservation Standard (ECS) of 3.73 lb/kWh, which conventional electric dryers were required to meet starting in June 2015. The three standard-size heat pump dryers save less than 20% of energy when compared to the ECS standard using the DOE Test Procedure for residential clothes dryers. Savings with other loads and settings will likely vary. Purchase prices were obtained from Internet searches. The only price found for the Kenmore dryer was from the Sears website². The best discounted prices for the others were obtained from U.S. Appliance³.

¹ See www.energystar.gov/products/appliances/clothes_dryers; CEF Measured according to the U.S. Department of Energy (DOE) test method for Clothes Dryers (10 CFR 430, Subpart B, Appendix D2).

² <http://www.sears.com/kenmore-elite-7.4-cu-ft-advanced-hybrid-dry/p-02681593000P?intcmp=ken-pdp-buy-cta>

³ <http://www.us-appliance.com/dryers.html>

Table 1.1. Heat pump clothes dryers in the U.S. residential market

Heat Pump Clothes Dryer	Vented?	Capacity ^a (cu-ft)	CEF ^a (lbs/kWh)	Energy Savings ^b	Drying Time ^a (min.)	Purchase Price ^c
Kenmore 8759	Y	7.4	4.3	13%	57	\$1,260
LG DLHX4072	Y	7.4	4.3	13%	58	\$1,145
Whirlpool WED99HED	N	7.4	4.5	17%	71	\$1,524
Blomberg DHP24412	N	4.1	5.7	55%	46	\$1,529

^a Data obtained from Energy Star website.

^b Energy savings calculated from DOE Energy Conservation Standard of 3.73 lbs/kWh.

^c Purchase price obtained during January, 2016 from Sears website for Kenmore and from U.S. Appliance website for others.

All three manufacturers of standard-size heat pump clothes dryers also market similar models that meet the ENERGY STAR requirement of 3.93 lbs/kWh (shown in Table 1.2). One consideration of a consumer deciding which dryer to purchase is the cost savings trade-off between higher purchase price and energy cost savings. A less than 5-year payback is generally required. The simple payback between a heat pump dryer in Table 1.1 and an equivalent ENERGY STAR model in Table 1.2 is shown in the last column of Table 1.2. The result of greater than 50 years for all three heat pump dryers is based on average annual energy use reported on the ENERGY STAR website and assumes 9.75¢/kWh electricity cost. Clearly a consumer would not decide to purchase one of the standard-size heat pump dryers based only on energy cost savings.

Table 1.2. Heat pump clothes dryer energy savings and simple payback when compared to similar ENERGY STAR electric (only) models

Heat Pump Clothes Dryer	Annual energy use (kWh) ^a	ENERGY STAR Model			Simple Payback (yrs) ^d
		Model ^b	Annual energy use (kWh) ^a	Purchase Price ^c	
Kenmore 8759	556	81582	607	\$873	78
LG DLHX4072	556	DLEX4270W	607	\$845	60
Whirlpool WED99HED	531	WED95HEDW	608	\$984	72

^a Annual energy use obtained from ENERGY STAR website.

^b Energy Star model from same manufacturer that is similar to heat pump clothes dryer model based on product description.

^c Purchase price obtained during January, 2016 from manufacturer for Kenmore and from U.S. Appliances website for others.

^d Based on incremental purchase cost divided by annual energy cost savings using difference in ENERGY STAR estimated annual energy savings and assuming 9.75¢/kWh electricity cost.

In many cases, higher costs of more efficient appliances are subsidized by utilities through rebates or by governments through tax incentives. Energy savings of around 15% may not be sufficient to justify an incentive program for heat pump dryers. New Jersey currently offers a \$300 incentive, but only for the Blomberg compact model. Puget Sound Energy is offering \$150 incentive for all heat pump dryers, which cuts the calculated payback of the LG heat pump dryer in half.

However, all of the dryers in Table 1.2 have met the criteria for the ENERGY STAR Emerging Technology award,⁴ which requires a minimum CEF of 4.3 lb/kWh in the ‘normal’ setting and at least 5.3 lb/kWh in at least one setting, as well as cycle completion in less than 80 minutes. The accompanying

⁴ Energy Star Emerging Technology award criteria can be found at https://www.energystar.gov/index.cfm?c=pt_awards.pt_clothes_dryers_advanced_dev.

label incentivizes consumers who perceive additional value in energy savings beyond monetary benefits, such as environmental consciousness, and are willing to pay the higher costs associated with this technology. It remains to be seen the level of success these products have in capturing market share. Clearly improvements in the technology in energy savings and payback will broaden the appeal and yield higher overall energy savings in the U.S.

Several attempts have been made in the past to develop heat pump dryers capable of significant energy savings. The DOE commissioned an effort in 2003 with TIAX and Whirlpool [6] to develop a heat pump dryer that would be marketable in the U.S. The prototype developed by TIAX was successful in achieving 40–50% savings with 35°F lower fabric temperatures and similar drying times as conventional dryers. The prototype also improved fabric temperature uniformity and exhibited robust performance across a range of vent restrictions. The approach that TIAX took was to shorten drying times by substantially increasing air flow from 100 cfm to about 250 cfm. They also changed the heat pump refrigerant to increase air temperature. The prototype required a larger blower and used heat exchangers as large as the available space within the dryer cabinet and pedestal base could accommodate. The higher air flow created issues with lint migration to the heat exchanger surfaces and cloth plastering onto the outlet grill of the dryer; however, these issues were overcome. The project was successful in meeting its goals of energy savings and comparable drying times and much of what was learned in that study was useful in this effort.

While TIAX took a variable venting approach, heat pump dryers available in the world market are ventless, recirculating the drying air in a closed-loop. Water is condensed from the moist warm air coming from the drum as the air is cooled by the evaporator of the heat pump. The condensate water is discharged into a drain. The air is then reheated by the heat pump condenser before returning to the drum. More heat is added to the air in the condenser than is removed from the evaporator. The difference is the heat of compression added by the heat pump compressor. The extra heat must be removed from the dryer with an extra heat exchanger and blower or fan to exchange heat between the recirculating air and the room air. A booster electric resistance heater is often used to shorten the drying time by adding additional heat at the start of the cycle to bring the load up to drying temperature more quickly. None of the documented efforts to develop heat pump dryers have used a heating element for supplemental air heating throughout the cycle.

Fortunately, dryer manufacturers with heat pump dryers available on the world markets have solved many of the challenges of these appliances. For example, water condensed from the dryer air must be accumulated and disposed of, such as through the wash machine drain line. Lint accumulation can be more problematic in the closed-loop recirculating heat pump dryers, because lint accumulating on heat transfer surfaces will degrade their performance. Lint accumulation on the optional booster heater is a fire hazard. The advantage of the proposed hybrid, vented concept is that the condenser and element components are up stream of the drum and never see air laden with lint. Provisions for maintaining the evaporator surfaces as well as the optional recuperative heat exchanger are required, similar to what is done with existing heat pump dryers.

1.3 Technical Approach

Understanding how energy is used in drying clothes is important for devising a technical approach for optimizing energy savings in a heat pump clothes dryer. To illustrate, Figure 1.2 shows power and cumulative energy consumption profiles of a drying cycle along with drum exhaust temperature and RMC of the load. These data were obtained from a commercial standard electric clothes dryer [1]. When a cycle starts, most of the energy is used to heat up the wet load, the heating elements, and the rest of the dryer, although some drying occurs from the start as illustrated by the decreasing RMC curve. The

beginning warm-up stage of a typical drying cycle is indicated on the left in Figure 1.2. Next, during the bulk drying stage, the exhaust air temperature normally stabilizes, the heaters are usually on continuously, and the exhaust air is at high relative humidity. This is also referred to as the constant rate drying process (CRDP) [7]. During the CRDP phase, there is very little sensible duty, and the latent duty of evaporating water consumes the energy. At the end of the CRDP phase, the latent duty decreases because evaporation of water decreases, which shifts the energy input to sensible duty, causing the dryer and load to heat and the exhaust temperature to rise (shown in Figure 1.2). This is also referred to as the falling rate drying process (FRDP) [7]. At this point, the dryer goes into a high heat phase, in which the heaters are modulated to prevent overheating of the load (see the power profile in Figure 1.2). Typically, there is a cool-down phase at the end in which the heaters are turned off to allow the clothes to cool before ending the cycle. With the heaters off, there is minimal energy used. A load is considered dry between 5% and 2% RMC, indicated by the vertical lines in Figure 1.2. In this example, the load is essentially dry at the end of the bulk dry phase and is over dried during the high heat phase, but this is not consistently observed [1]. The increase in RMC during the cool-down phase is indicative of over-drying during the high heat stage.

The drying process and how the energy is being used changes substantially between the three phases. In the warm-up stage, energy is split between heating the dryer components—heaters, drum, and rest of the cabinet contents—and drying the load. The latter is supported by the drop in RMC, which starts at 57.5% at the outset in the DOE Test Procedure and can decrease to 35–40% by the end of the warm-up phase [1]. The warm-up stage is consistently 30–40% of the energy consumption for standard dryers corresponding to 30–40% of the total latent duty, which implies that the inefficiency of heating up the dryer and load is not a large parasitic energy cost. Almost all of the energy is used for drying during the bulk drying phase, where 30% up to almost 60% of the total energy is used. While the division of energy consumption between the phases varies with load and dryer settings, as well as how the transitions are determined, the overall pattern is consistent between different dryer models tested [1].

Most of the ‘work’ of drying the load is performed in the first two phases, but up to a third of the total energy used can be consumed in the last high heat phase [1]. Essentially, the function of the last phase is to ensure the load is dry at the end of the cycle, which is critical for consumer satisfaction. The cycles must consistently achieve perceived dryness for a wide variety of load sizes, cloth types, and mixtures. Despite contact moisture sensors located in many dryers, there is a tendency for algorithms in dryers to over dry the loads [2].

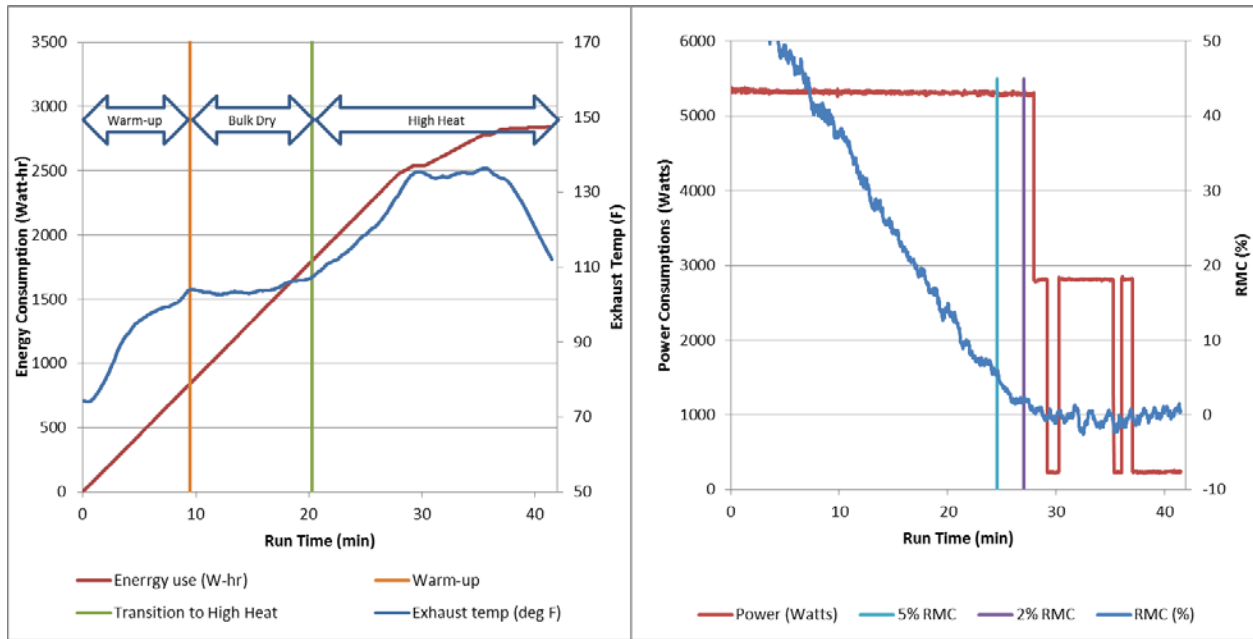


Figure 1.2. Example of warm-up, bulk dry, and high heat (combined with cool-down) stages of an automatic termination cycle from testing of Test Unit 1 with the AHAM 1992 load on COTTONS and high temperature settings; the power profile on the right shows when one or both heating elements are on along with the RMC data obtained from the scale measurements.

The technical approach used for designing a HyHPCD started with developing a model of the drying process through the three drying stages. The model is validated using data from an off-the-shelf standard-size vented electric dryer. After incorporating a heat pump system, the model is used to design a heat pump that will yield at least 50% energy savings over the entire cycle. This design is then implemented in a demonstration system by modifying the electric dryer that was used for validating the model. The modified electric dryer is then tested in an environmental chamber following the DOE Test Procedure. Energy usage data from extensive previous testing of the unaltered electric dryer provides a baseline for computing energy savings with the HyHPCD.

The next section describes the computational model and the process of designing the HyHPCD. Section 3.0 describes the implementation of the demonstration system and provides test results. Section 4.0 concludes with a discussion of progress made on achieving energy savings and the potential for improvements relative to the demonstration system.

2.0 Hybrid Heat Pump Clothes Dryer Design

The design of a HyHPCD was accomplished with a computational model. First, a model was developed for a conventional electric clothes dryer, in order to accurately reflect the drying process occurring in the drum through the three phases of a drying cycle. The approach for demonstrating the technology was to retrofit an off-the-shelf electric clothes dryer with a heat pump system. Therefore, the first step was to calibrate the conventional dryer model to data acquired for the selected dryer. Next a model was developed for the HyHPCD that incorporated a heat pump system. This second model served as the tool for designing the demonstration system.

2.1 Conventional Electric Clothes Dryer Model

The clothes dryer model utilizes ChemCAD, a commercial process simulation software package, to perform heat and mass balance calculations at a given instant of time in the cycle. The dynamics of the drying process are calculated in an Excel spreadsheet that utilizes the ChemCAD flowsheet that is shown in Figure 2.1. Inlet air first passes through the element representing the resistance heating element. The sink unit operation (7) is used to simulate the thermal mass of the heating element, drum, and dryer load. Heat is removed or added to the air by the sink when thermal mass is being heated or cooled during the warm-up and high heat stages of the drying cycle. During the CRDP when temperatures are not changing, the sink is set to zero. The drum unit operation (8) is a mixer where liquid water added to the air evaporates, which represents the drying process inside the drum. The moist air from the drum is then exhausted. An algorithm was developed for each of the phases of the drying cycle described above, which also determines when the heating elements are turned on and off.

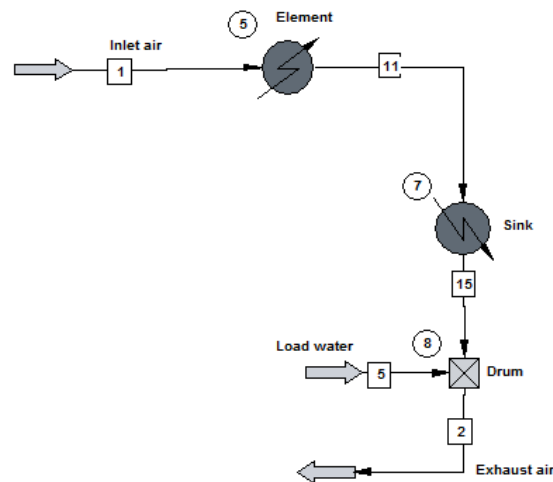


Figure 2.1. ChemCAD flowsheet of a conventional electric dryer

Unknown parameters of the model, including air flow rate and thermal masses, are fit using data obtained from a dryer that has been selected for demonstration of the HyHPCD concept. The parameters are obtained from heat balances and the thermal response at the beginning warm-up and the high heat drying phases. A method for setting the drying rate, which varies through the cycle, is also required.

Data from a test with the selected electric drying using an AHAM 2009 test load [8] on high temperature and normal dryness settings are used to calculate the unknown parameters for the selected electric dryer. PNNL conducted tests in an environmental control chamber with the ambient temperature

and RH controlled to 75°F (23.9°C) and 46%, respectively. The load mass was 3.80 kg and RMC was 57.52%, or 2.184 kg of water. The dryer has two elements; when subtracting the blower and drum motor power of 162 Watts, the two elements drew 2,640 and 2,500 Watts. At times, only the first higher power element was on.

Air flow rate is created by a centrifugal blower located after the drum, which produces a relatively constant volumetric flow of dryer exhaust. This means the mass flow of air changes with temperature and RH of the drum exhaust. During the constant drying rate process, temperatures are stable, so all of the heater power is going to evaporate water and heat the ambient air to the exhaust temp. An energy balance during the CRDP is written as

$$E_e = \lambda_{w@T_e} (\dot{n}_{w,e} - \dot{n}_{w,i}) + \dot{n}_a \int_{T_i}^{T_e} C_{p_a} dT + \dot{n}_{w,i} \int_{T_i}^{T_e} C_{p_w} dT \quad (2.1)$$

where E_e is the element power, λ_w is the latent heat of vaporization for water, \dot{n} is molar flow, C_p is molar heat capacity, subscripts w and a refer to water and dry air, respectively, and subscripts e and i refer to the exhaust and inlet streams, respectively. The drum and load are assumed to be at the exhaust temperature in Equation 2.1. Assuming the ideal gas law, the total exhaust volumetric flow rate is

$$Q_{T,e} = \frac{P}{RT_e} (\dot{n}_a + \dot{n}_{w,i} + \dot{n}_{w,d}) = \text{const.} \quad (2.2)$$

where the subscript d refers to the water evaporated from the load. The measured relative humidities and temperatures of the inlet and exhaust streams provide relationships between the dry air flow and water flows in the feed and exhaust streams, respectively. Combining relative humidities with equations 2.1 and 2.2 enables the calculation of the exhaust volumetric flow during the CRDP.

This calculation was performed for the selected dryer from a test performed using an AHAM 2009 test load [8], as well as high temperature and normal dryness settings of the dryer. For this case, the exhaust air flow was calculated to be 119 CFM, while the dryer's technical manual states the maximum dryer air flow is 150 CFM.

Integrating the drying rate, $\dot{n}_{w,d}$, over the entire cycle assuming constant volumetric flow of the exhaust and using the RH and temperatures of the inlet and exhaust streams gives the total amount of water removed from the load. Numerically integrating the total mass of water evaporated gives

$$m_{T,w} = MW_w \sum_{j=1}^{Np} (\dot{n}_{w,e} - \dot{n}_{w,i})_j \Delta t_j \quad (2.3)$$

where Δt is the time step between measured data points and the sum is over the entire cycle. For the same AHAM 2009 load as above, the total water removed was calculated to be 2,235 g, while the difference in the measured weight of the load was 2,154 g between the start and end of the cycle test, representing a 3.8% error.

The thermal mass that must be heated and cooled is comprised of the dryer, the load, and the load moisture content, the latter of which changes during the drying cycle. In lieu of a very detailed thermal analysis of the dryer thermal mass, the model assumes two thermal masses. Drying air is assumed to be adiabatically heated by the element power before entering the drum, and the corresponding final

temperature is one characteristic temperature. The heating element and nearby components, such as the heater cowl and back of the drum, can reach this temperature; this represents one thermal mass. The drum exhaust temperature is the second characteristic temperature, and the load, drum, blower, and exhaust ducting are assumed to track with the drum exhaust temperature. More detailed analysis of thermal masses requires additional data, such as temperature measurements and the masses and heat capacities of dryer components. However, these two thermal masses are able to effectively account for thermal transients during the warm-up and FRDP phases of the drying cycles.

The two thermal masses are determined from thermal analysis data obtained for the selected dryer. The first part of the FRDP phase is used to compute a 'drum' thermal mass, because the heaters have been fully on for at least 15 minutes, so the 'heater' thermal mass is at a relatively constant temperature. The exhaust temperature is steadily increasing, so the drum thermal mass is heating up along with the load and remaining moisture. Therefore, a heat balance during this part of the cycle can yield the drum thermal mass. The power from the heating elements minus the heat of vaporization, heat loss in the air, and the heating of the load and moisture is attributed to the drum thermal mass. This is obtained by numerically integrating the heat balance equation

$$E_e = \lambda_{w@T_e} M_l \frac{dRMC}{dt} + \int_{T_i}^{T_e} (\dot{n}_a C_{p_a} + \dot{n}_{w,i} C_{p_w}) dT + (C_{th,l} + C_{th,w} + C_{th,d}) \frac{dT_e}{dt} \quad (2.4)$$

in time from the start of the high heat phase until a heater is turned off for the first time, and solving for the drum thermal mass, $C_{th,d}$. Air temperature is T , and subscripts i and e refer to inlet and drum exhaust respectively. Heat of vaporization of water at the exhaust temperature is $\lambda_{w@T_e}$, and M_l is dry weight of the load. Subscripts a , w , l , and d refer to dry air, water, load, and dryer, respectively, and \dot{n} , C_p , and C_{th} are molar flow, heat capacity, and thermal mass. The data collection frequency was 1 Hz, so one second is the time step for numerical integration. The heat of vaporization is calculated from the load mass times the change in RMC, which is determined from the scale weight of the dryer and contents. The heat loss to the air is the same as the last two terms in Equation 2.1. Heating of the load thermal mass, $C_{th,l}$, uses the dry load weight and the heat capacity of cotton cloth, 1.3 J/g.K. The remaining moisture thermal mass, $C_{th,w}$, is also calculated from the RMC.

For the same test with the AHAM 2009 load used to calculate an air flow of 119 SCFM, the net energy adsorbed by the thermal masses when the exhaust temperature was increased from 107°F to 128°F was 546.5 kJ. Of this, the load adsorbed 56.7 kJ and the remaining moisture only 1.0 kJ, because the RMC was low. The remaining energy attributed to heating the drum is 488.8 kJ. Using the heat capacity of steel at 0.49 kJ/kg.K, the mass of the drum heated from 107°F to 128°F is 191 lbs (87 kg). This drum weight is unrealistic because the dryer weight reported in the product literature is 115 lbs. However, it is likely that the change in average temperature of the drum materials is greater than the change in exhaust temperature, which would reduce the calculated drum mass. Therefore, the drum thermal mass of 42.6 kJ/K is used in the dryer model to account for thermal energy stored and released by the machine as the exhaust air temperature changes during the warm-up, FRDP, and cool-down stages of clothes dryer cycles.

During the warm-up phase, both the drum and the heater thermal masses are heating up in addition to drying and heat losses in the exhaust air. The heat balance equation, Equation 4, applies during the warm-up phase, with the addition of the heater thermal mass, $C_{th,h}$, to the last term.

Again using the same test data, the exhaust increases from 74°F to 92°F during the first 4 minutes with thermal masses consuming 714 kJ, including 418 kJ for heating the drum, 48 kJ for heating the

clothes, and 86 kJ for heating water, leaving 161 kJ for heating the ‘heater’ thermal mass. Assuming the heat thermal mass is steel and heats to the adiabatic heating temperature of the incoming air, which is 224°F at 4 minutes into the cycle, the mass of the heater is 8.7 lbs or 1.94 kJ/K thermal mass.

The model requires an algorithm for setting the drying rate, represented by the water flow into the drum (Stream 5) in Figure 2.1. Theoretically, water can be evaporated from the load until the drying air is saturated or is at 100% RH. RH values as high as 80–100% have been measured during the CRDP when the load RMC is high. The model sets the drum exhaust RH to a constant value during the CRDP.

As the load becomes dry and the cycle enters the FRDP, the drying rate falls precipitously. At this stage, the drying rate is no longer constrained by the water carrying capacity of the air, but by the mass transfer of water out of the clothes. Figure 2.2 shows the drying rate plotted against the load RMC during the same test with the AHAM 2009 load that was used to compute air flow and thermal masses above. The FRDP part of the cycle, highlighted in red, shows how drying rate slows when the RMC drops below about 20%. The red highlighted data in Figure 2.2 are fit to the quadratic equation shown in Figure 2.2, and this equation is used to set the drying rate during the FRDP in the model.

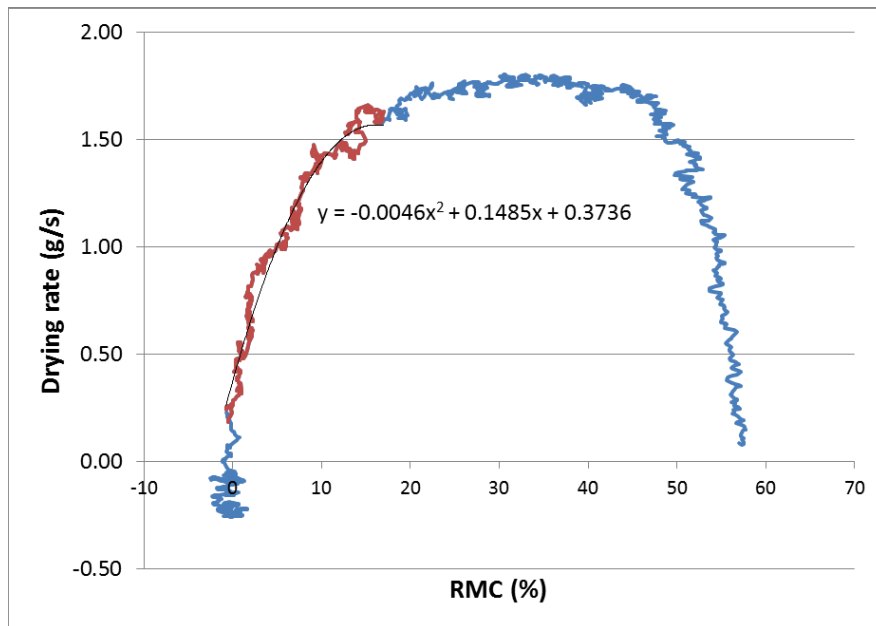


Figure 2.2. Quadratic fit of drying rate to RMC during the FRDP phase of a drying cycle

During the warm-up phase, the drum exhaust starts at the ambient temperature and RH; both increase as the drum and load warm. The drying rate is initially very low (but non-zero) because there is little capacity for water in the exhaust at ambient temperature. The drying rate increases steadily with the exhaust temperature and RH until the cycle enters the CRDP phase. Figure 2.3 shows the drying rate plotted against the exhaust temperature minus the ambient (chamber) temperature during the same test with the AHAM 2009 load that was used previously. The warm-up phase is highlighted in red showing the gradual increase in drying rate as the drum warms, and the highlighted data are fit to a linear equation that is used to set the drying rate during the warm-up phase in the model.

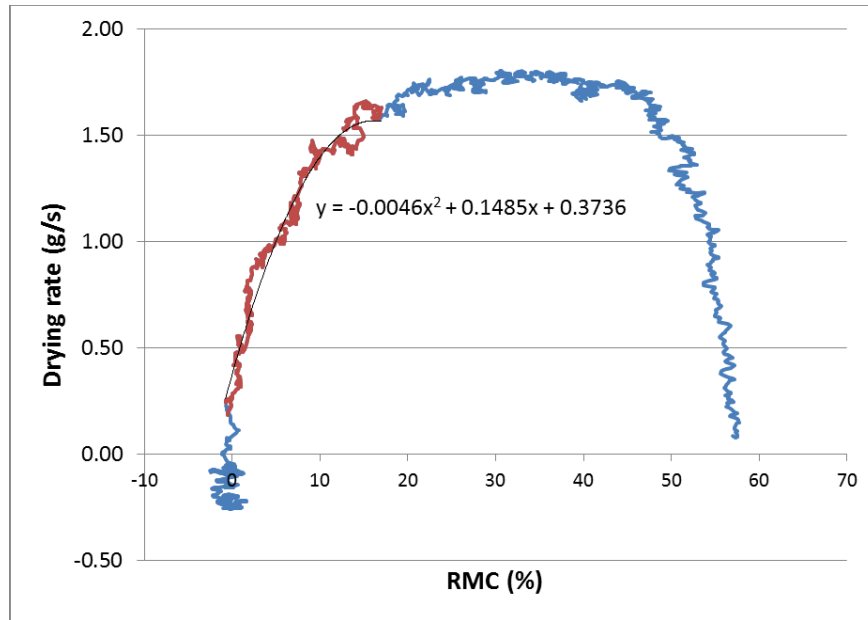


Figure 2.3. Fit of drying rate to $(T_{\text{exhaust}} - T_{\text{ambient}})$ during the warm-up phase of a drying cycle

In summary, the volumetric flow of exhaust is kept constant during the entire drying cycle, and the model includes two thermal masses—the ‘heater’ thermal mass that tracks with the temperature of the drying air entering the drum and the ‘drum’ thermal mass that tracks with the temperature of the exhaust air. The volumetric flow of the exhaust and the size of the thermal masses are input parameters to the model. The model divides the drying cycle into three phases—a warm-up phase, a CRDP, and a FRDP. The drying rate during the warm-up phase uses a quadratic function of the difference between the exhaust and ambient temperatures. The model transitions to the CRDP when the exhaust reaches a prescribed temperature of around 38°C (100°F). Setting the exhaust RH to a fixed value sets the drying rate during the CRDP. Once the load RMC reaches a set level, the model transitions to the FRDP, where the drying rate is now a linear function of the RMC until the load is dry (zero RMC).

The other input to the model is an algorithm for turning the heaters on and off. Typically, heaters are modulated to prevent overheating of the load using an algorithm specific to a dryer’s control system which is undisclosed by the manufacturer. Meanwhile, the cycle is continued with the load at temperature for some period to insure the clothes are dry. The temperature of the final phase of the drying cycle is emulated with the model to fully account for the energy consumption of an electric dryer.

2.2 Drying Cycle Simulation of an Electric Dryer

A simulation of the electric dryer selected to be modified for the HyHPCD demonstrator was completed in order to accurately reflect the drying process occurring in the drum and to validate model parameters, which could then be incorporated into a model of the HyHPCD. The HyHPCD model would then be more reliable in predicting energy savings, resulting in a more optimized design.

Data were used from a drying cycle that used an AHAM 2009 test load with the dryer set on normal dry and high temperature settings. The test was performed in an environmental chamber at an average temperature of 23.9°C (74.9°F) and 47.4% RH. The bone dry weight of the test load was 3.80 kg (8.36 lbs) and the starting RMC was 57.5%. The power of one heating element was 2,640 Watts and the second was 2,500 Watts. These parameters were all obtained directly from measurements during testing.

Other parameters had to be calculated from the data as described above. The blower flow rate was determined to be 56.4 L/s (120 cfm) based on energy balances. The thermal masses of the ‘heater’ and ‘drum’ were 1,945 J/K and 42,581 J/K, respectively. The drying rate during the warm-up phase was a linear function of the difference between the drum exhaust and ambient temperatures.¹ The model transitioned from the warm-up phase to CRDP when the exhaust temperature reached 37.8°C (100°F). During the CRDP, the drum exhaust RH was maintained at a constant 80%, and the model transitioned to the FRDP when the RMC reached 21.8%.

The drying rate during the FRDP was a quadratic function of the RMC, which is given in Figure 2.2. Turning heaters off and on was started when the exhaust temperature reached 54.4°C (130°F). The use of heaters for the rest of the cycle emulated the original test. The 2,640 Watt heater was operated alone for 75 seconds followed by no heaters for 64 seconds. The 2,640 Watt heater was then used for 5 minutes, off for 46 seconds, and then back on for 58 seconds. No heaters were used after that point. When no heaters were on, an arbitrary 200 Watts of heat was extracted from the heater thermal mass to continue heating the incoming air.

Comparisons of the simulation results to the measured test data are shown in Figure 2.4 and Figure 2.5. The shape of the exhaust temperature and RH curves are in agreement with the measured data, as is the drying rate as represented by the RMC in Figure 2.5. The simulated cycle reached 130°F during the FRDP approximately one minute earlier than the actual cycle after which it followed the same heater cycling, so the energy consumed in the simulated cycle is slightly less than in the actual cycle. These results serve as a validation that the drying process in the drum is reasonably accurate.

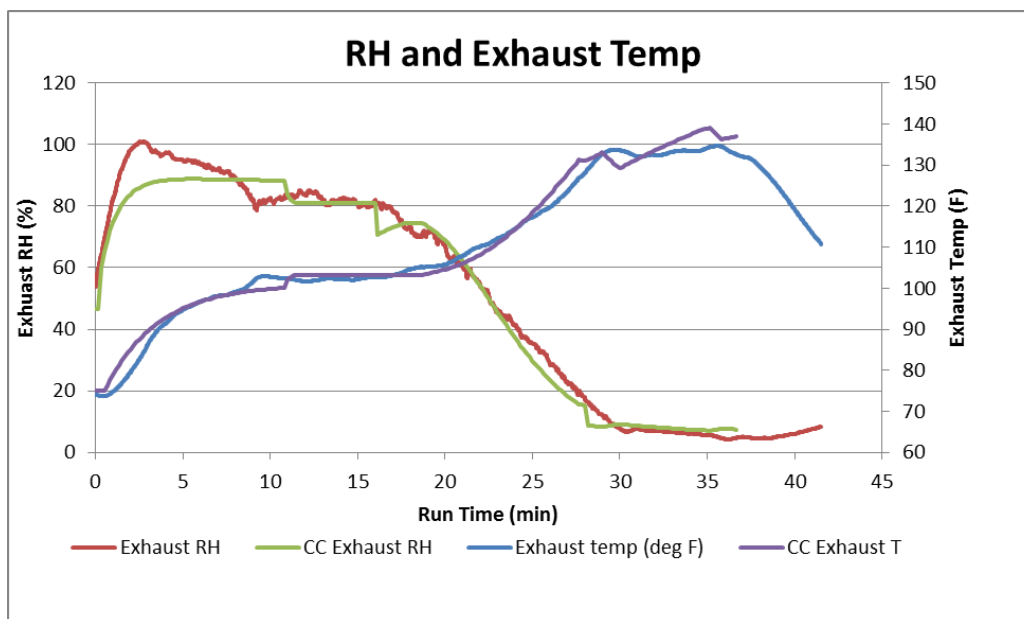


Figure 2.4. Comparison of exhaust RH and temperatures between the ChemCAD simulation (CC) and the experimental measurements

¹ The warm-up drying rate equation was $F_w = 0.1086 * (T_{exh} - T_{amb}) + 0.226$, where water flow rate, F_w , is in g/s, and T_{exh} and T_{amb} are the exhaust temperature and the ambient temperature in °C, respectively. Note, the intercept was reduced by half from the linear fit described in Section 2.1, in order to obtain a better fit of the RMC and exhaust temperature curves.

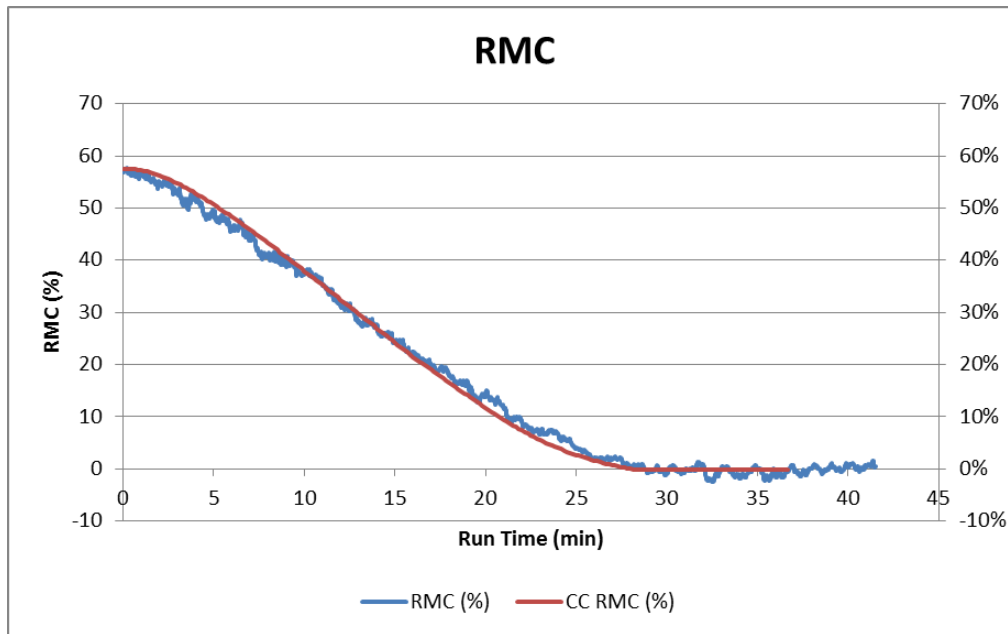


Figure 2.5. Comparison of RMC between the electric dryer model (CC) to the experimental measurements of the AHAM 2009 test

2.3 Hybrid Heat Pump Clothes Dryer Model

The HyHPCD model incorporates the electric dryer model, which includes an Excel spreadsheet that utilizes the ChemCAD flowsheet shown in Figure 2.1. The heat pump system is represented by the additional unit operations that are shown in Figure 2.6. The compressor, condenser, evaporator, and expansion valve (TXV) are the typical components of a vapor compression heat pump used in a refrigerator or air conditioner. The reason the condenser is split into two heat exchangers (Unit Ops 1 and 10) is explained below. The recuperative heat exchanger (Rec HX, Unit Op 6) is also included to preheat the incoming air by recovering heat from the drum exhaust. The water separator is included for the convenience of tracking the amount of water that is condensed from the drum exhaust. The condensate water will need to be collected in a sump and pumped to a drain, but the water pump is not represented in the model.

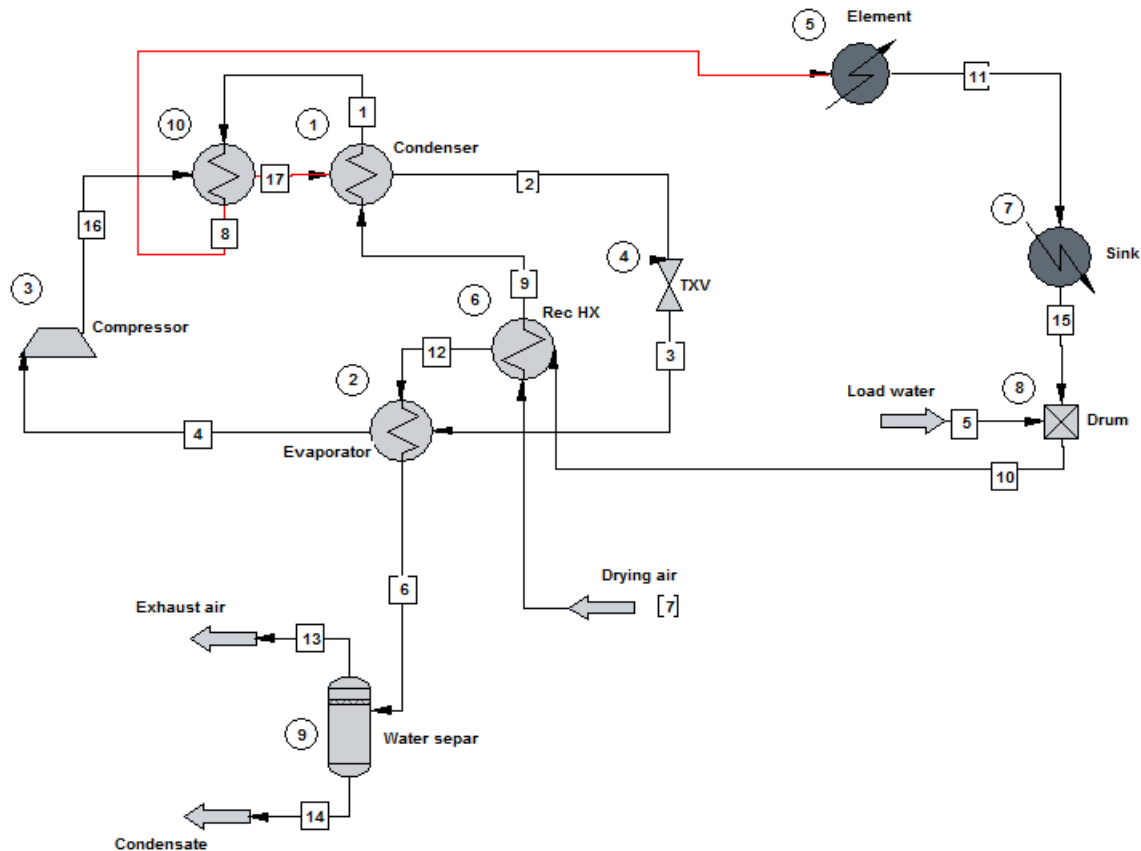


Figure 2.6. ChemCAD flowsheet of a hybrid heat pump clothes dryer

The model sets the high and low side pressures of the refrigeration cycle with specifications for the compressor (3) and expansion valve (4), respectively. The high side pressure is set by specifying the outlet pressure of the compressor. The low side pressure is specified by setting the bubble point of the refrigerant exiting the expansion valve.

Standard off-the-shelf tube-fin heat exchanger coils are anticipated for the evaporator and condenser components. The recuperative heat exchanger is expected to be a plate-frame style. These are single- or multi-pass cross-flow style heat exchangers, but the version of ChemCAD used has only co-current and counter-current heat exchanger choices. Therefore, the evaporator is specified as a co-current flow heat exchanger in the model, which is not overly constraining because the refrigerant side is mostly phase change at nearly a constant temperature. The co-current model is overly constraining for the recuperative heat exchanger, so the counter-flow model is used but specified so that a single-pass cross-flow heat exchanger can be utilized.

The condenser is split into two heat exchangers to take advantage of the superheat in the refrigerant coming from the compressor to heat the air to a higher temperature. The first heat exchanger (Unit Op 10) is modeled as a counter-flow exchanger, but is specified so a multi-pass tube-fin coil can be used. The second heat exchanger (Unit Op 1) is a phase change heat exchanger that is mostly isothermal on the condensing side, so it is modeled as a co-current flow exchanger.

The heat exchangers are specified with a constant heat transfer coefficient, U , and heat exchanger area, A , with the exception of the first part of the condenser, Unit Op 10. Instead, the model sets the

outlet temperature of the refrigerant stream to a value slightly higher than the condenser saturation temperature, T_c , at the high side pressure.

The two remaining parameters needed to specify the operation of the heat pump are the refrigerant flow and the compressor efficiency, which are both determined from the performance ratings of the compressor selected in the heat pump design. The Air-Conditioning, Heating, and Refrigeration Institute has a standard for rating compressors [8] that specifies a method for using a polynomial equation to correlate power input, mass flow rate, current, and compressor efficiency (or cooling capacity) to the suction dew point and discharge dew point temperatures for a given refrigerant. The correlation for mass flow rate is used to specify the refrigerant flow in the heat pump loop of the model. Similarly, the compressor efficiency in the model is selected to match the power consumption in the model to the power input correlation for the compressor.

A thermostatic expansion valve (TXV) is typically used in a vapor compression heat pump to modulate the refrigerant flow in order to maintain superheat in the evaporator discharge to prevent liquid carryover from the evaporator into the condenser suction. The amount of superheat in the evaporator discharge is a target parameter in the model. The bubble point at the expansion valve outlet is changed iteratively until the evaporator superheat calculated from the ChemCAD solution is within tolerance of the target.

The volumetric flow rate through the blower is assumed constant, so the air entering the drum depends on the temperature and added amount of water in the air coming out of the evaporator. The additional water in the drying air is the difference between the water added by the drying process and the water removed by condensation in the recuperator and/or evaporator. The specified air flow into the drum in the ChemCAD model is changed iteratively to keep volumetric flow through the blower at a constant value within a tolerance.

The phases of the drying cycle and the transitions between phases are governed by model parameters. During the start-up of the warm-up phase, all the heat in the air goes to heating the 'heater' thermal mass up to temperature. The sink power in the ChemCAD model is modulated so the temperature of the air entering the drum (Stream 15) is at the ambient temperature. When the heater is up to temperature, which is typically less than a minute, the drum begins to receive heated air that heats the drum and load thermal masses as well as beginning the drying process. During the remaining period of the warm-up phase, the sink duty in the ChemCAD model (Unit Op 7) is matched to the increase in sensible heat of the heater, drum, and load thermal masses. The model transitions into the CRDP when the drum exhaust temperature reaches a value determined by a parameter.

During the CRDP, the RH of the drum exhaust air is maintained at a set level, and the CRDP ends and the FRDP begins when the load RMC reaches a set value. The heater is turned off during the FRDP when the exhaust temperature increases to a set temperature. The compressor remains on to keep the load hot for an additional period of time. The timing is used to approximate the thermal profile of the drying cycle of the original electric dryer to ensure the load is at a comparable dryness at the end of the cycle.

2.4 Hybrid Heat Pump Clothes Dryer Design

The most important consideration in the design of the HyHPCD was using off-the-shelf components, defined as items both currently available on the market or readily customized conventional technology that would be readily available. The overall goal of the design was 50% energy savings with a comparable drying time to the original electric dryer. Payback is also a consideration but wasn't used at this stage of the design.

The component that was most challenging to select was the compressor. Heat pump compressors on the market are intended for consumer products, such as refrigerators and air conditioners, where the heat is rejected at ambient conditions. Therefore, the operating range of most compressors has an upper limit of 50–65°C for the condensing temperature. However, the HyHPCD model indicated a higher condensing temperature is needed in order to obtain enough heat from the heat pump to save 50% of the energy. Special requests were made to several compressor companies for higher temperature machines. Private communications with a technical contact at Embraco identified model FFI12HBX-EJ as one that could be taken to a 70°C (158°F) condensing temperature with R-134a refrigerant, even though it was rated to only 65°C (149°F). Consequently, the Embraco compressor was selected with R-134a as the refrigerant, and the condensing temperature was kept constant at 70°C throughout the cycle.

Through modeling of the HyHPCD, it was discerned that the air should be heated to about 80°C (176°F) in the condenser to meet the objectives. The innovation that enabled this was the two-stage condenser shown in Figure 2.6; this condenser utilizes the superheat in the refrigerant from the compressor to heat the drying air above the condensing temperature. Super Radiator Coils, the supplier of the condenser and evaporator heat exchangers for the demonstration, confirmed that this configuration was possible in a multi-pass, cross-flow tube-fin coil.

The finalized design for the HyHPCD demonstration incorporated the Embraco Model FFI12HBX-EJ, utilizing correlation coefficients provided by Embraco to calculate refrigerant flow and input power from the evaporating and condensing (saturation) temperatures. The superheat from the evaporator was set to 8.3°C (15°F), and the evaporating temperature was allowed to fluctuate, as described above. The recuperator heat transfer coefficient and area were 35 W/m²-K and 3.6 m², respectively, and were 25 W/m²-K and 12 m² for the evaporator. The second part of the condenser was modeled with a 30 W/m²-K heat transfer coefficient and an area of 12 m². The constraint on the desuperheating section of the condenser was an outlet refrigerant stream temperature of 71.5°C (161°F), which prevented an internal pinch but allowed the size of the heat exchanger to fluctuate slightly.

The parameters that were common with the electric dryer model were kept the same, including thermal masses of the heater and drum and the blower volumetric flow rate at 119 CFM. Drying rate was calculated the same throughout the cycle. Ambient temperature and RH were 24°C (75°F) and 46%, respectively, as before. The warm-up phase was ended when the drum exhaust reached 37.8°C (100°F), at which point the drum exhaust was kept at 80% RH during the ensuing CRDP. The cycle then transitioned to the FRDP when the load RMC reached 21.8%. These parameters were chosen to emulate the performance and drying process of the electric dryer that was incorporated into the demonstration system.

A single heater element is included in the HyHPCD model, and the power was adjusted to give a comparable drying time to the original electric clothes dryer. This was achieved with a heater power of 1,760 Watts, compared to 5,100 Watts in the original electric dryer. A drying time similar to the original dryer was established by the drum exhaust temperature profile, which is shown in Figure 2.7. The heater is turned off part of the way through the FRDP and only the heat pump is used to reach the peak drum exhaust temperature of ~57°C (135°F). The heat pump is not as effective as a heater during the warm-up phase, so the initial rise in temperature is slower, but eventually gets to the same exhaust temperature for the CRDP phase. At this point, the recuperator continues recycling heat to the incoming air, which results in a slower cool-down. The advantage is that power is not consumed to heat the air in the last stage of the drying cycle, which results in significant energy savings. On the other hand, the load is 12°F warmer at the end of the cycle.

Figure 2.8 shows the load RMC profiles through the cycle. The slower warm-up causes a lag in the RMC curve for the HyHPCD, but the slope is comparable. Tests with electric dryers show considerable

variability in the load final RMC between tests, and the final RMC varies between types of loads [1]. The model simply dries the load until the RMC reaches zero. By keeping the load hot for an additional period of time and continuing to operate through a cooldown phase, there is high confidence that the load will reach the same level of dryness as was reached in similar cycles with the original electric dryer.

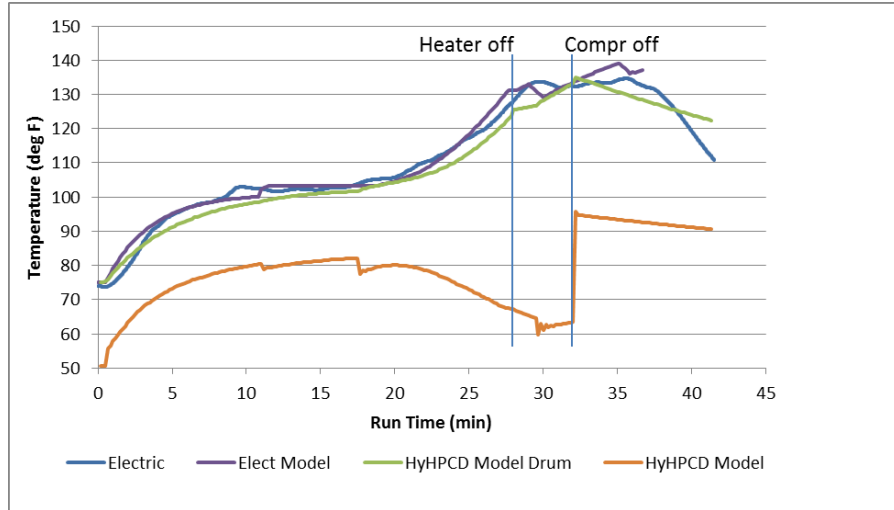


Figure 2.7. Comparison of exhaust temperatures between the original electric dryer data, the electric dryer model results, and the HyHPCD model results, including both drum exhaust and evaporator exhaust for the HyHPCD. Vertical lines indicate when the heating element and compressors were turned off.

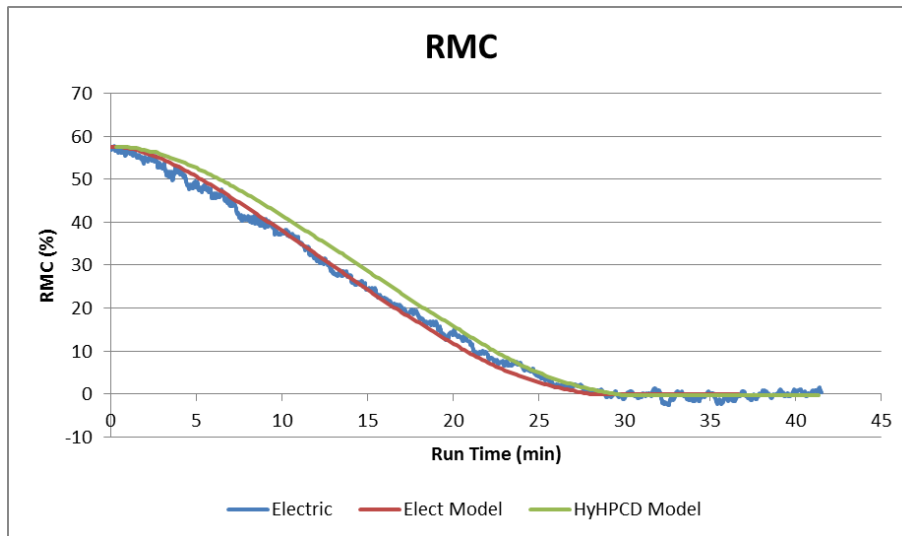


Figure 2.8. Comparison of RMC profiles between the original electric dryer data, the electric dryer model results, and the HyHPCD model results

The run-time for the HyHPCD cycle is 41.3 minutes compared to the electric dryer test that lasted 41.5 minutes. The electric heater and compressor consume 1.23 kWh. The original electric dryer consumed 2.84 kWh, of which 0.16 kWh was used by the blower running at 234 Watts on average. Therefore, the HyHPCD saved 54.3% of the energy used to heat the air, not including the blower power. If the same blower power is assumed for the HyHPCD and it is added to the overall electricity consumed, the savings for the HyHPCD drops to 51.2%. In reality, the blower power will need to increase to accommodate the added pressure drops of the heat pump system. The increase in blower power is

unknown and depends on the heat exchanger designs, but if it is assumed that the blower power doubles, the energy savings drops to 45.5%. Therefore, the HyHPCD design that is defined within the model is capable of achieving the desired 50% energy savings at a comparable drying time.

The energy savings with the HyHPCD is strongly dependent on the recuperative heat exchanger, because it is a passive device that recycles heat with no increase in power except for a modest increase in blower power. Figure 2.9 illustrates the energy profile of the HyHPCD. At the beginning of the cycle until the system warms up, the majority of heat added to the air comes from the element and none comes from the recuperator. The recuperator contribution is modest all the way through the CRDP, but increases as the exhaust temperature rises in the FRDP until it provides all of the heating at the end of the cycle. The ability to continue heating the incoming air after power is shut off to the heat and heat pump allows those to be turned off earlier while still guaranteeing a dry load. This leads to dramatic energy savings at the end of the cycle, enabling the system to achieve 50% energy savings.

This is further illustrated in Figure 2.10, which shows the efficiency of heating the drying air, defined as

$$\eta = 1 - \frac{P_e + P_c}{H_r + H_{hp} + H_e} \quad (2.5)$$

where P_e and P_c are the heating element and compressor power, respectively, and H_r , H_{hp} , and H_e are the heat duties of the recuperator, heat pump condenser, and heater element, respectively. This efficiency indicates how much more heating is achieved over the power that is being consumed, not including the blower motor. The metric is useful for tracking energy savings, because in order to achieve 50% energy savings over the entire cycle, the efficiency must average over 50%. An electric dryer always has an efficiency of zero, because $P_e = H_e$ and the other terms are zero. The lower efficiency during the warm-up phase in Figure 2.10 is more than compensated by the high efficiency at the end of the cycle when the recuperator alone is heating the air with no power, which enables the desired 50% overall energy savings.

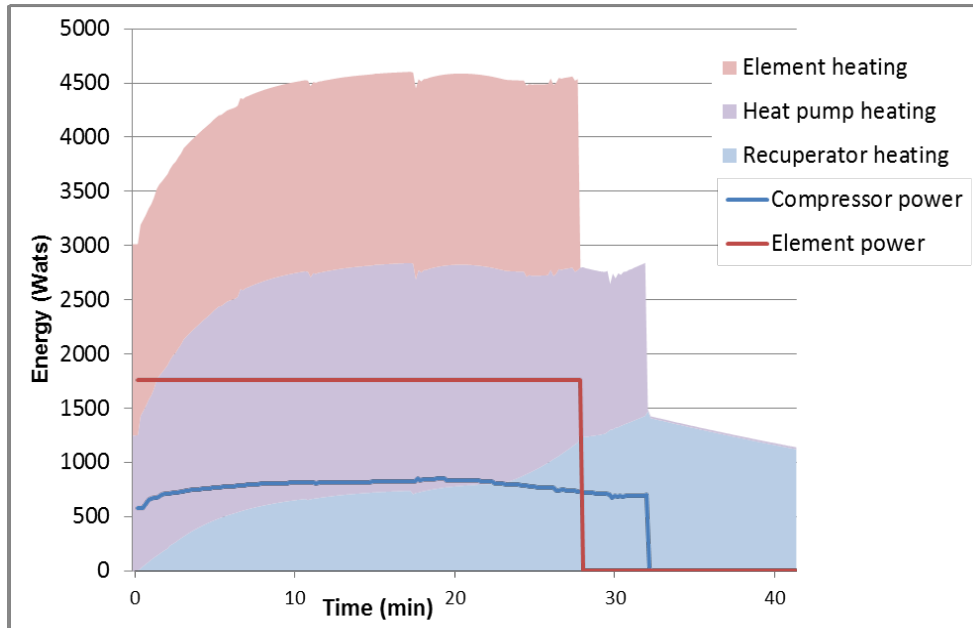


Figure 2.9. Energy profile of the HyHPCD model results, including power inputs to the compressor and element, overlaid on a stacked-chart of the heating of the incoming air by the recuperator, the heat pump, and the electric element.

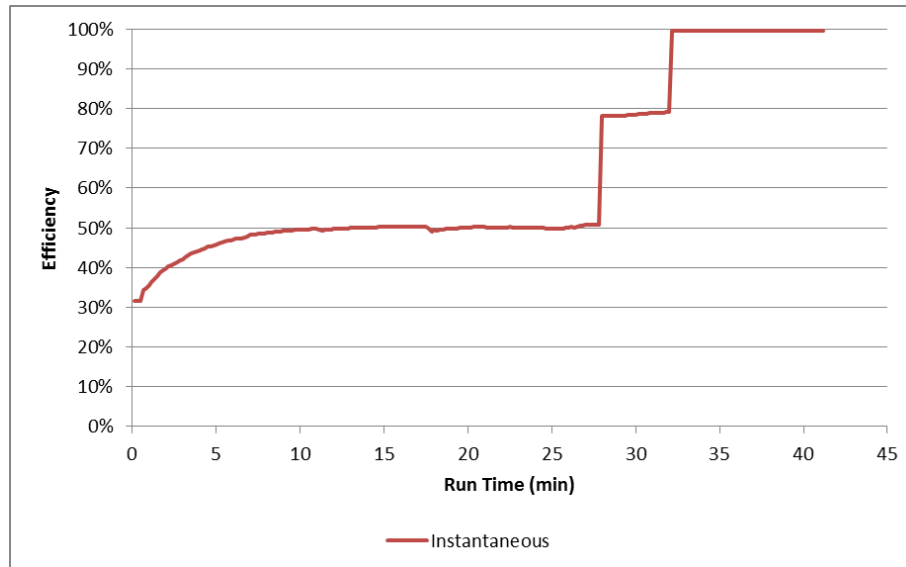


Figure 2.10. Efficiency of heating the drying air during the drying cycle of a HyHPCD

The EF obtained for the HyHPCD design based on the model is 6.0 lbs/kWh with the AHAM 2009 load, assuming the blower power is the same. If the blower power doubles, the EF reduces to 5.4 lbs/kWh. The CEF values for the three standard-size HPCDs in Table 1.2 are 4.3-4.5 lbs/kWh, so this design represents a step change in energy savings for clothes dryers. Furthermore, the drying cycle with our design is complete in 42 minutes in comparison to 57-71 minutes for the HPCDs in Table 1.2. Consequently, our design is able to raise energy savings from less than 20% to over 45% with a much shorter cycle time.

3.0 Demonstration of Hybrid Heat Pump Clothes Dryer

3.1 Components and Assembly

A GE Model GTDN550ED standard vented electric dryer, which was available from a previous project at PNNL, was modified and used for the demonstration of the HyHPCD. The GE dryer as delivered, shown in Figure 3.1, was previously tested extensively, so baseline data are available that can be used for calculating energy savings [1]. The GE dryer was modified for the demonstration that included sealing all holes and cracks to prevent air from leaking into or out of the cabinet and insulation was added to the interior of cabinet walls. The dryer controls were disabled and a National Instruments control system with a Labview interface was created to support operation of the HyHPCD as well as for data acquisition. Consequently, the original dryness sensor and auto termination algorithm were unavailable, and the HyHPCD was operated and terminated manually, which is described in the next section. The original dryer heating elements located at the back of the drum were used, but the electric power supplied to the heaters was lower than the original 240 VAC. The power to one heater was either 145 VAC or 120 VAC which corresponded to 1000 Watts or 700 Watts, respectively, when it was on. The power to the second heater was 640 Watts at 120 VAC and could be modulated lower in the control system by reducing the percent of time it was on—a setting of 40% meant the second heater was powered for 2 second and then off for 3, for example. The cabinet of the dryer was also modified to interface to the heat pump system.



Figure 3.1. GE Model GTDN550ED standard vented electric dryer that was instrumented, placed on a scale for measuring RMC, and tested following the DOE Test Procedures in a previous PNNL project [1].

Heat pump components were specified based on system modeling results that indicated at least 50% energy savings, as described above. Specifications for the heat exchangers were provided to multiple heat exchanger vendors who were asked to quote volumes of 1, 10, and 1000 units. The latter quantity was used for the payback analysis that is described in the next section. Super Radiator Coils was selected to provide conventional tube-fin heat exchangers for the condenser and evaporator components. HeatEx was selected to provide a stacked-plate heat exchanger for the recuperator; two sizes of heat exchangers were ordered. Pictures and technical information for the heat exchangers are included in Appendix A. The Embraco Model FFI12HBX-EJ compressor was used, and a picture and information are also provided in Appendix A. The Parker/Sporlan EFJ-1/2 was selected for the thermostatic expansion valve and a sightglass was also installed in the refrigerant loop to facilitate charging.

The goal was to operate the HyHPCD with approximately the same air flow through the drum as the GE electric clothes dryer. To overcome the added pressure drop of the heat exchangers, two Tjernlund Model LB1 booster blowers were added at the inlet before the recuperator intake and at the outlet of the evaporator. Eventually, the original dryer blower would be combined with the booster blowers for a single higher power blower with less overall power consumption. Consequently, the booster blower power was not included in the power metering.

The heat pump system was designed to be located under the original electric dryer as shown in the CAD drawings in Figure 3.2. This configuration mimics packaging the heat pump subsystem in the pedestal of a standard dryer. The CAD drawing of the heat pump system is shown in Figure 3.3. Plenums were constructed from 20 gauge stainless steel sheet metal to duct the air flow between the heat exchangers. Air flows into the recuperator as indicated in Figure 3.3, through one side of the recuperator, turns 90° upward, and flows through the condenser oriented horizontally, as specified by the vendor. The air from the condenser passes through a hole cut in the bottom of the dryer cabinet. A baffle installed in the cabinet around the drum just behind the drum motor confines the air to the back of the cabinet where it flows past the electric heaters and into the back of the drum. Figure 3.4 shows the original dryer cabinet with the drum removed and a baffle and insulation added inside the cabinet. The original internal air duct from the blower to the back of the dryer was removed and replaced by a flexible 4-inch duct, also shown in Figure 3.4, that directs the air from the blower to a hole in the bottom of the cabinet. The air flows through the 4-inch round hole, through a plenum, and through the other side of the recuperator, as shown in Figure 3.3. Lastly, the air flows through the evaporator and the booster blower (not shown).

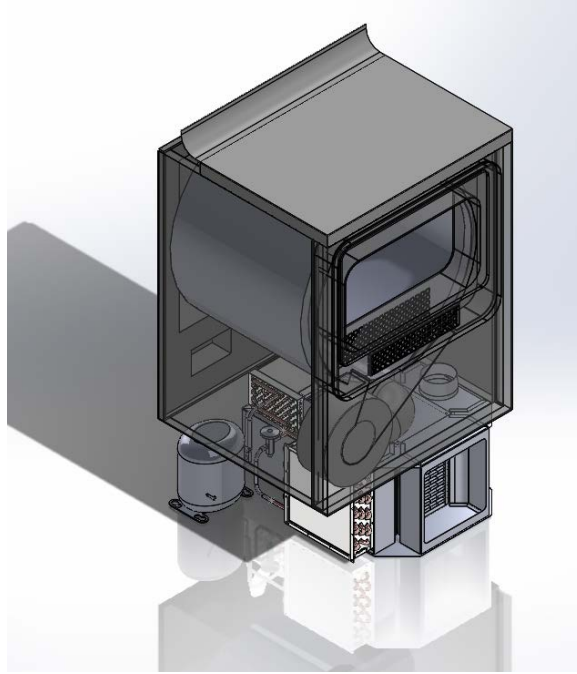


Figure 3.2. CAD drawing of the GE Model GTDN550ED standard vented electric dryer on top of the heat pump system.

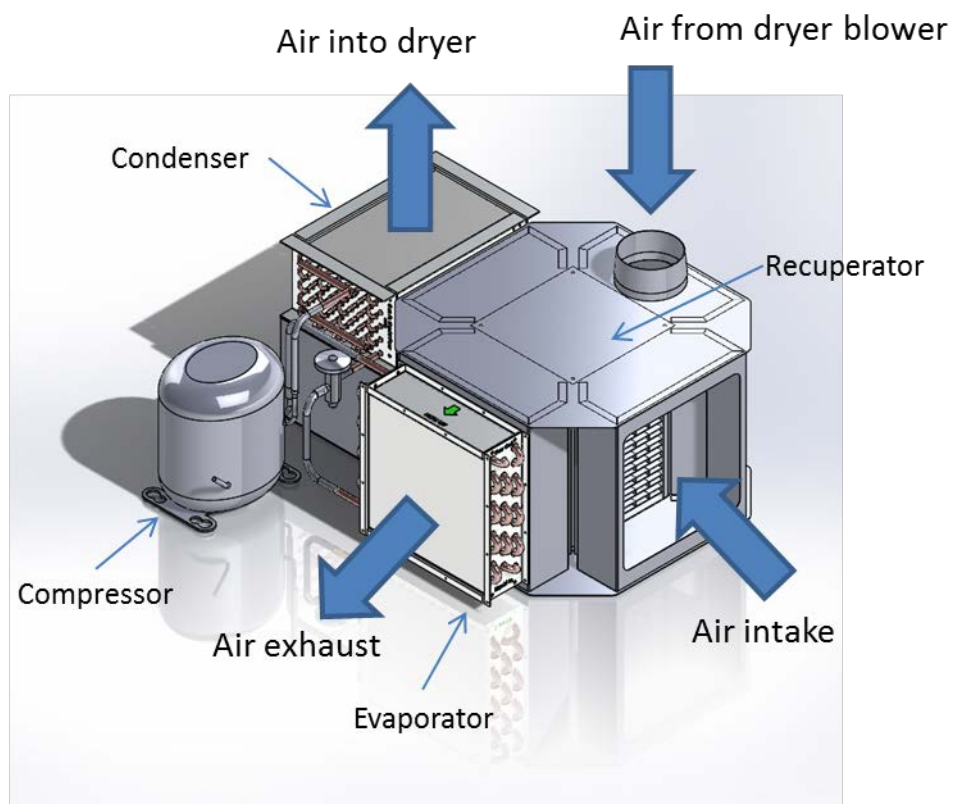


Figure 3.3. Heat pump CAD design

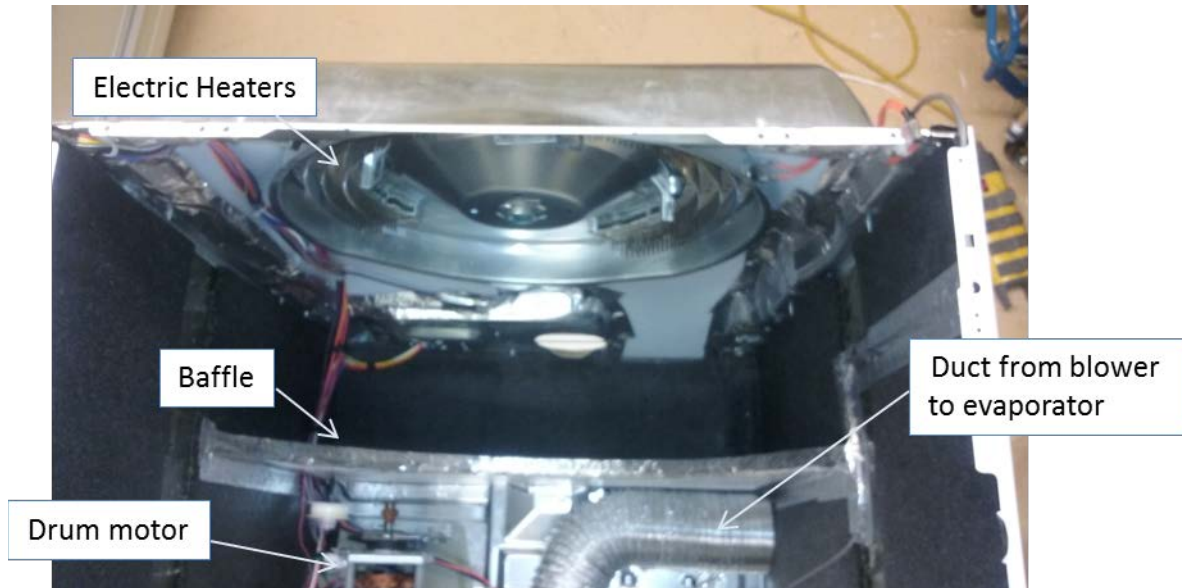


Figure 3.4. Dryer cabinet with drum removed showing added baffling and insulation and the internal duct from the blower

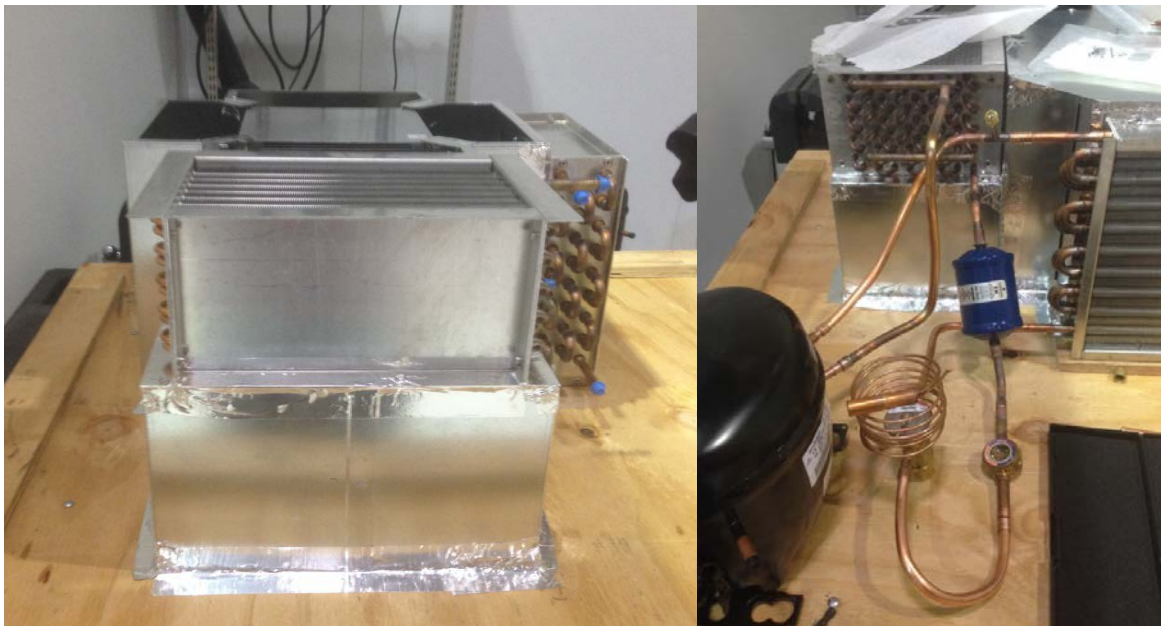


Figure 3.5. The heat pump subsystem during the assembly process; heat exchangers with interconnecting plenums on the left and the refrigerant loop on the right

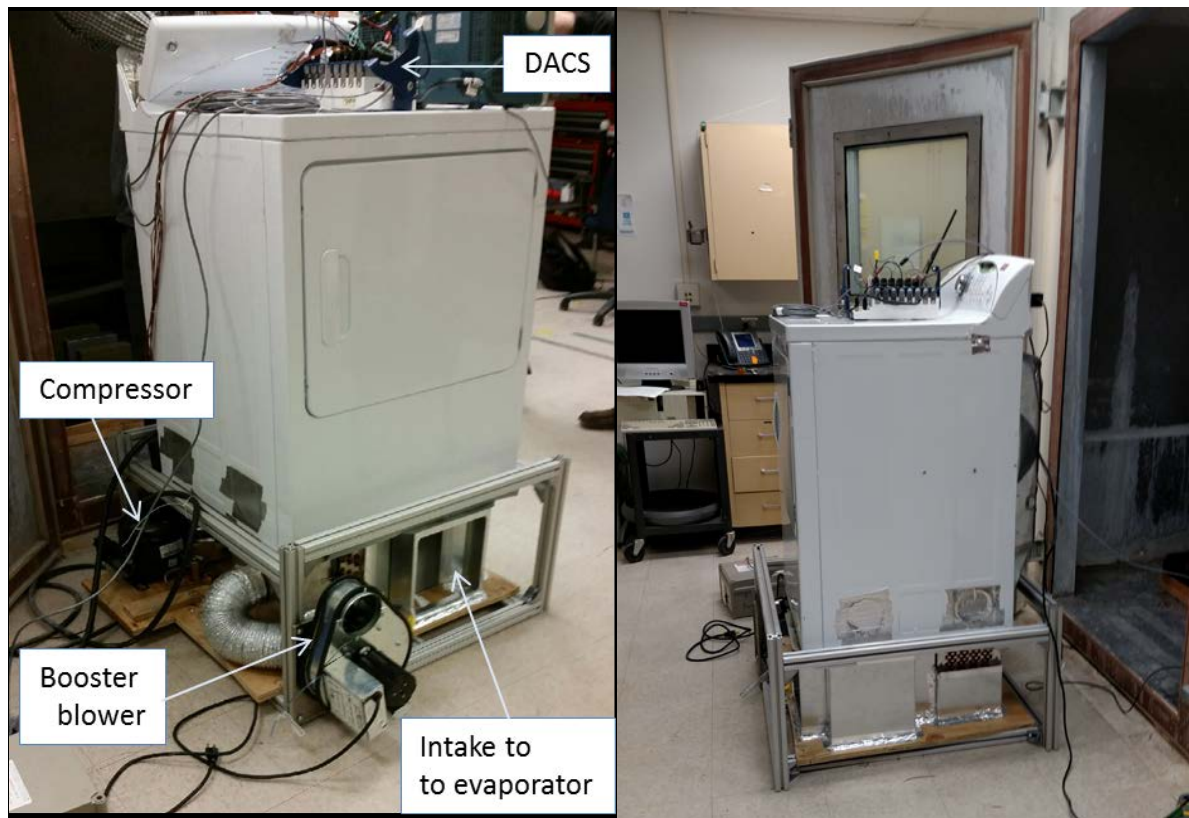


Figure 3.6. The HyHPCD system next to the environmental chamber used for testing

Pictures of the HyHPCD demonstration system are shown in Figure 3.5 and Figure 3.6. Jabil constructed the heat pump subsystem shown in Figure 3.5. The left picture shows the assembly of the heat exchangers with the interconnecting air plenums. The horizontally oriented condenser is in front on top of the plenum connecting it to the recuperator behind. The evaporator is located behind to the right of the recuperator. Figure 3.6 shows the fully assembled HyHPCD demonstration system. The National Instruments data acquisition and control system (DACs) system is located on top of the dryer. The flexible ducting is shown connecting the outlet of the evaporator to the booster blower in the picture on the left. A side view is shown in the picture on the right with the environmental chamber used for testing behind the dryer.

3.2 Data Acquisition and Control and Test Procedure

The DACs consisted of National Instrument equipment and Labview software for the man-machine interface (MMI) and data logging. The HyHPCD demonstration system was manually controlled through the MMI. A button on the control screen started and stopped the drum motor that started the dryer blower and the drum rotating. Other buttons started and stopped the heaters and the heat pump compressor. One heater was always at full power when turned on while the other could be modulated by entering the percent on into a field on the MMI. This allowed the heat power to be varied between tests, but a fixed heater power was used throughout a given test. The auxiliary blowers were not operated through the MMI, but were simply plugged into a 110 VAC outlet.

Interlocks were programmed into the control system as safety features. The heaters could not be powered unless the dryer door switch indicated it was closed and the drum motor was on. Dryer safety features, such as thermal fuses, were incorporated in the control system. Overheating the dryer was

prevented by setting an upper limit on the drum exhaust temperature that automatically turned off the heaters. Similarly, an upper limit was set on the temperature of the compressor discharge to protect the compressor from overheating. The compressor also had a temperature switch that shut off the compressor and prevented restarting until the compressor cooled.

Monitoring and recording power consumption was necessary to determine total power use during a drying cycle test in order to calculate energy savings. One power meter measured the combined power consumption of dryer motor and heaters. The second power meter monitored compressor power consumption. The accuracy of the power meters were $\pm 1\%$. The DACS also summed both power measurements over the entire cycle from when the drum motor was first started until it was turned off to obtain total energy consumption of the cycle.

Several other instruments were used to monitor the system, and measurements were recorded every one second by the DACS. Dwyer combined temperature and RH probes were used for monitoring the ambient air and the drum exhaust. Thermocouples were placed in the drying air stream at the inlet to the recuperator, the inlet and outlet of the condenser, and the inlet and outlet of the evaporator. The drum exhaust RH probe was used to calculate the water content of the exhaust air, which was assumed constant until the air was cooled to the saturation temperature. Thermocouples were placed in contact with the outer wall of the refrigerant piping to monitor refrigerant temperatures before and after the condenser and evaporator. Thermocouples were also placed in contact with the housings of the compressor and blower motor. The latter was added when it was discovered that the blower motor was running hotter than normal, as high as 57°C , and above the nameplate temperature of 40°C . The on/off status of the dryer motor, heaters, and compressor were also recorded every 1 second.

The procedure used for testing the HyHPCD system followed the DOE D2 Test Procedure [3] as closely as possible. Details of the equipment and procedures used for measuring the bone dry weight, preparing a test load, running a test, measuring final RMC, and data analyses can be found in TeGrotenhuis [1]. The HyHPCD system was installed in an environmental chamber to maintain room conditions at $75 \pm 3^{\circ}\text{F}$ and relative humidity at $50 \pm 10\%$, as required by the test procedure. This was confirmed by an RH probe located inside the chamber. While the HyHPCD model was developed using test data from an AHAM 2009 test load [8], testing were performed using the standard DOE test load defined in the DOE D2 Test Procedure or with the AHAM 1992 test load [8]. A test load of the prescribed mass was bone-dried and loaded with water to the required starting RMC by following the test procedure. The dryer was cooled after the bone-drying procedure, as required. After recording the bone dry and starting RMC, the test clothes were loaded into the dryer, and the button was pressed on the DACS to start the drum rotating and the dryer blower, which marked the start of the cycle. The compressor and heater(s) were started at this point, which completed the start-up of the cycle into the warm-up phase.

The DOE D2 Test Procedure [3] for automatic termination control requires the dryer to be operated with the 'normal' or 'cotton' program, the temperature setting set to maximum, and the dryness selected for 'normal' or 'medium'. The cycle is allowed to run to completion of the programmed cycle. The final RMC of the load must be less than 2% in order to be a valid test. An automatic termination cycle has not been developed for the HyHPCD, so these requirements of the test procedure cannot be met at this time. Instead, the heaters and compressor were operated to emulate the exhaust temperature profile of the original GE electric dryer and to reach the required final RMC. The heuristic that was used turned on the heater and compressor at the start of the cycle and powered them through the warm-up phase. The CRDP started when the drum exhaust temperature stabilized. We use the term 'EXPRESS' as the operating mode designed to minimize drying time, and both the heater and compressor were operated throughout the CRDP in EXPRESS mode. The term 'ECO' designates those tests designed for higher energy savings while trading-off for longer drying times. In ECO tests, the heater was turned off and only the

compressor ran through the CRDP. The start of the FRDP occurred when the rate of increase in drum temperature noticeably increased, at which point the heater was turned off, leaving the compressor to heat the air during the FRDP. The drum exhaust temperature was allowed to increase to a certain value, at which point the heat pump was also turned off, leaving only the drum motor operating for the cool-down phase. Cool-down was typically around eight minutes, at which point the dryer was stopped, the load was removed from the drum, and the load was weighed to the nearest gram to determine final RMC. The specifics of the heuristic algorithm were varied to ensure the load was sufficiently dry at the end of the cycle.

3.3 Test Results

The objective of the testing is to determine energy savings of the HyHPCD relative to the baseline energy consumption of the original unaltered electric dryer. Most of the tests were performed with the standard DOE test load, and a few tests were performed with the AHAM 1992 test load. The DOE test load provides a measure of energy savings using a standard test and enables direct comparison to HPCDs that are currently on the market. The AHAM 1992 test load is more representative of real-world loads with a wider variety of cloth types and weights. Baseline data were obtained for the original GE dryer in a previous PNNL project from three duplicate D2 tests with both test loads [1]. The three duplicate tests with the DOE test load gave an average EF of 3.22 lbs/kWh, had an average cycle time of 40 minutes, and reached an average final RMC of 0.58%. With an AHAM 1992 load, three duplicate tests yielded an average EF of 3.27 lb/kWh, an average cycle time of 37 minutes, and an average final RMC of 1.53%. These results are used to evaluate the performance of the HyHPCD.

The 15 tests performed with the HyHPCD are shown in Table 3.1. Three tests were performed with the AHAM 1992 test load and the rest with the standard DOE test load. The power to the electric heaters was varied between 500 Watts and 1000 Watts. Both the heater and the heat pump were started within 20 seconds of starting a test, and were shut off at different times depending on the heuristic being applied to a given test. During ECO tests, heaters were used only for warm-up, and heaters were used through the entire CRDP during the EXPRESS tests. In ECO tests, the heaters were turned off after the drum exhaust temperature stabilized, typically 4 to 7 minutes into the cycle. If the heaters were used throughout the CRDP, the goal was to turn the heaters off when the drum exhaust temperature began increasing more quickly, indicated by an inflection in the temporal curve. The compressor was left running during the FRDP until the drum exhaust temperature increased about 10°C (40°F) after the heaters were turned off. The average drum exhaust temperatures during the CRDP are included in Table 3.1, along with the drum temperature when the heaters and compressor were turned off.

Table 3.2 shows the results of the 15 tests listed in Table 3.1. The results show that all but two of the tests achieved a final RMC below 2% as required by the DOE D2 Test Procedure. The EF values calculated from the measured weight of the load and the amount of energy consumed are included in Table 3.2. Energy savings are relative to the average EF obtained from the original electric dryer for the same test load. All but one test with the AHAM 1992 load achieved at least 40% energy savings. The goal of at least 50% energy savings over the baseline electric dryer was achieved in three ECO tests with the DOE test load. The energy savings relative to the DOE 2015 energy conservation standards, also included in Table 3.2, are lower because the original electric dryer was manufactured prior to the new 2015 Federal ECS and thus did not meet the new ECS standard of 3.73 lb/kWh. The HyHPCD exhibited energy savings of over 30% relative to the new 2015 ECS in all of the valid tests with the DOE standard test load.

However, the goal of comparable drying times was not met with the HyHPCD. Drying times were 30–50% longer with the DOE test load with the EXPRESS mode tests and 60–90% longer in the ECO

mode tests. Nevertheless, drying times were comparable or shorter than the commercial heat pump clothes dryers currently on the market and with considerably higher energy savings.

The results are compared graphically in Figure 3.7 to the performance of the baseline electric dryer (red square), commercial standard-size heat pump dryers (green triangles), and the target performance (open circle). All of the results compared favorably to heat pump dryers currently on the market, with a substantially higher EF representing 16–33% additional energy savings at comparable drying times. Greater energy savings were obtained with longer drying times in ECO mode, as expected, but not in all cases. The targeted energy savings were achieved only in ECO mode with the DOE test load at the higher final RMC levels that still met the DOE D2 Test Procedure requirements.

Table 3.1. Tests performed with the HyHPCD demonstration system indicating test load used (A1992 indicates AHAM 1992 load), nominal heater power, when the heaters and heat pump compressor were turned off, and drum exhaust temperatures

Test	Type	Test load	Nominal Heater Power (Watts)	Heater off (min.)	Heat pump off (min.)	CRDP Drum T (°C)	Heater off T (°C)	Compressor off T (°C)
1	EXPRESS	DOE	1000	34.2	42.2	38.9	40.9	46.0
2	ECO	DOE	1000	5.0	57.4	33.4	31.9	43.2
3	EXPRESS	DOE	500	32.6	43.6	36.3	36.7	38.5
4	ECO	DOE	1000	5.7	60.4	33.4	34.7	46.2
5	EXPRESS	DOE	700	44.1	47.4	37.3	38.7	51.9
6	ECO	DOE	1000	5.8	60.5	33.5	33.3	48.3
7	ECO	A1992	1000	4.3	62.2	34.2	35.9	46.7
8	EXPRESS	A1992	700	39.4	57.5	38.4	42.2	51.9
9	ECO	A1992	1000	6.7	59.5	35.2	37.6	45.9
10	EXPRESS	DOE	700	39.4	43.8	38.3	40.3	46.9
11	ECO	DOE	700	4.2	54.3	36.4	37.0	46.2
12	EXPRESS	DOE	500	43.8	50.6	37.2	39.0	48.9
13	ECO	DOE	700	5.6	56.1	34.1	36.4	44.9
14	EXPRESS	DOE	500	43.9	52.1	36.5	37.7	53.0
15	ECO	DOE	900	37.2	42.9	38.8	40.5	50.5

Table 3.2. Test results including the load RMC at the end of the test, calculated EF, energy savings relative to the baseline dryer and the DOE ECS, and the drying time

Test	Type	Final RMC (%)	EF (lbs/kWh)	Energy Savings	Savings vs ECS	Drying Time (min.)
1	EXPRESS	1.07	5.40	40%	31%	50.8
2	ECO	1.18	6.42	50%	42%	65.0
3	EXPRESS	1.29	5.92	46%	37%	58.4
4	ECO	0.57	6.07	47%	39%	67.7
5	EXPRESS	0.68	5.33	40%	30%	55.0
6	ECO	0.81	5.84	45%	36%	68.5
7*	ECO	3.53 ¹	6.08	46%	39%	70.3
8*	EXPRESS	1.14	4.88	33%	24%	65.4
9*	ECO	3.52 ¹	6.19	47%	40%	67.1
10	EXPRESS	0.81	5.78	44%	35%	51.5
11	ECO	0.94	6.73	52%	45%	62.3
12	EXPRESS	0.84	5.80	44%	36%	57.9
13	ECO	0.97	6.64	52%	44%	64.1
14	EXPRESS	0.66	5.62	43%	34%	59.5
15	ECO	0.71	5.51	42%	32%	50.8

*Test performed with AHAM 1992 test load instead of DOE test load

¹Invalid D2 test because the requirement of less the 2% final RMC was not met

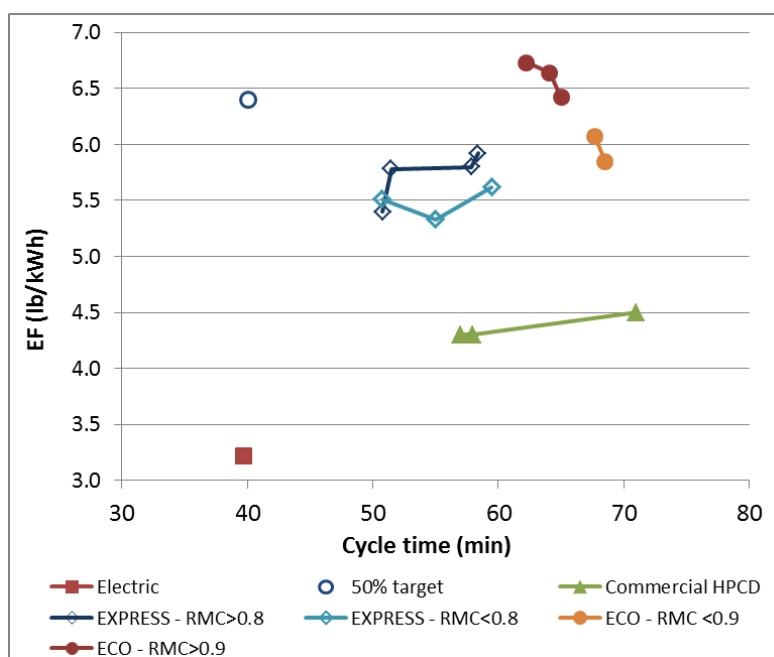


Figure 3.7. Comparison of results with the DOE test load to the original electric dryer, the 50% savings target, and commercial standard-size heat pump dryer; data are divided between higher and lower final RMC for the ECO and EXPRESS modes

Figure 3.8 to Figure 3.11 show measurement data from Test 10, an EXPRESS test that achieved 44% energy savings over the baseline and took 51.5 minutes with the DOE test load using a 700 Watt electric heater. Figure 3.8 shows the sequence of heating and cooling the drying air. Blue tones are used to illustrate the air up stream of the drum, which started at 21–24°C from the test chamber, was heated to over 30°C by the recuperator (Cond in), before being heated to over 70°C by the condenser of the heat pump after the warm-up phase. The electric heater heats the air further (not shown) before entering the

drum. The red tones in Figure 3.8 are down stream of the drum, where the air is progressively cooled as heat is recovered into the incoming air. The drop to the drum exhaust temperature is due to the conversion of sensible heat to latent heat in the drying process. The decrease from about 40°C to almost 30°C typically reaches the saturation temperature of the exhaust, resulting in condensation in the recuperator. For significant parts of the cycle, the evaporator is able to decrease the exhaust temperature below ambient while condensing a significant fraction of the water vapor.

Even after the heat pump is shut off at about 45 minutes, the air continues to be preheated by the recuperative heat exchanger. This attribute allows the heat pump to be turned off earlier while energy is still being provided to the drum to complete drying of the load. Electric dryers typically cycle the heaters during the FRDP to maintain temperature of the load for a period of time to ensure dryness, which can now be accomplished with passive heat exchange from the recuperative heat exchanger. This attribute contributes significantly to the overall energy savings, as illustrated by Figure 2.10.

The relative humidity of the drying air is shown in Figure 3.8 in the environmental chamber and in the drum exhaust. The test procedure requires the ambient air to be kept between 40% and 60% relative humidity throughout the test. Figure 3.8 shows this is accomplished for Test 10 within the chamber. The drum exhaust RH peaks during the warm-up phase, gradually decreases through the CRDP, and drops precipitously during the FRDP due to drying process slowing. The drum exhaust is at lower RH than the chamber because it is at higher temperature. Drying begins immediately when air flow is started even before the heater or compressor can provide heat, which causes the dip in exhaust temperature in Figure 3.8 due to evaporative cooling.

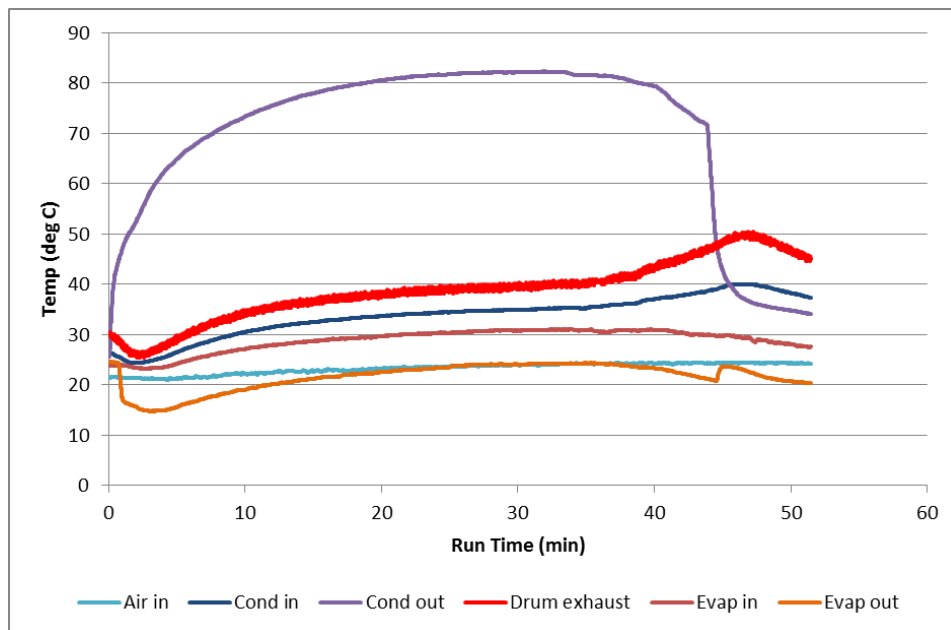


Figure 3.8. Temperatures of the drying air through the cycle for Test 10

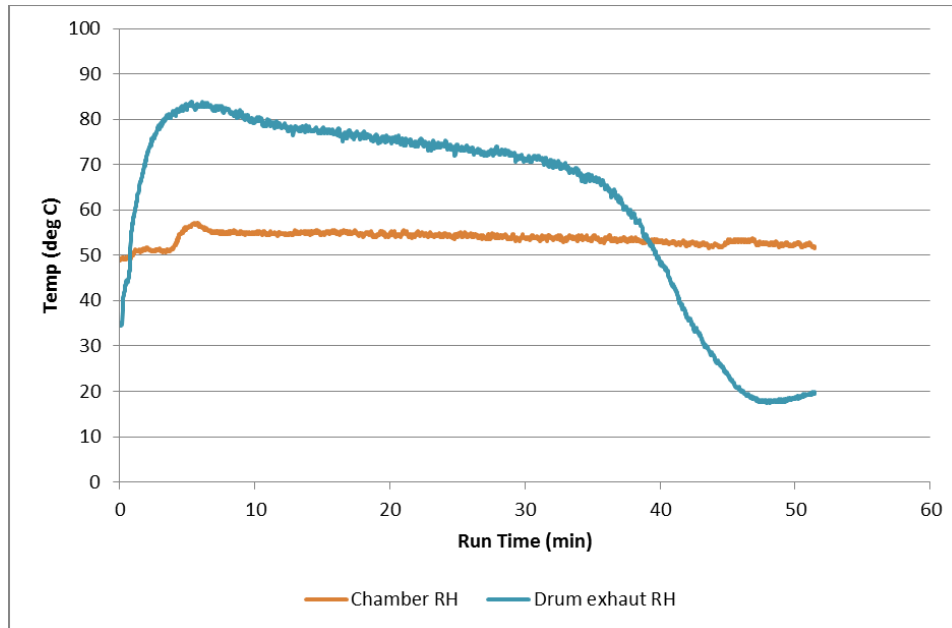


Figure 3.9. Relative humidity of the drying air through the cycle for Test 10

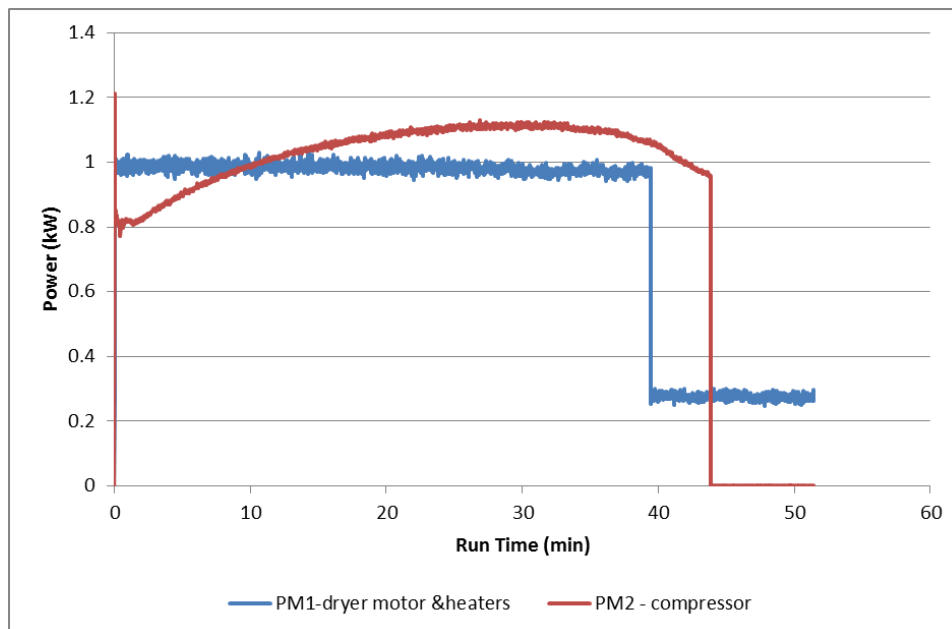


Figure 3.10.Power consumption of the compressor and combined heaters and drum motor through the cycle for Test 10

Figure 3.10 shows power consumption during the Test 10 drying cycle. One power meter, PM1, monitors the combined power used by the heaters and the drum motor. The period after the heater(s) are turned off gives the drum motor power use alone, which is assumed to be constant throughout the cycle. The average power used after the heater(s) are turned off is subtracted from the total to obtain the heater power. The second meter, PM2, monitors compressor power alone, which increases gradually through the CRDP as the temperature climbs and decreases during the FRDP, indicating the heat pump duty is also decreasing. The average power consumption of the heaters and compressor are tabulated in Table 3.3, along with the total energy consumed. The breakdown of energy consumption between the heater, compressor, and motor is also provided. Less than 10% of the energy is used by the heaters in the ECO

tests, but the motor energy increases due to the longer drying times. There is an optimization to be performed between heater power, heater use, and drying time, which has not been completed. Because the drying times are much longer than expected, the energy used by the motor during the cycle is higher than anticipated from the design, which is detrimental to energy savings.

The effect of heater power on EF is shown in Figure 3.11. As expected, higher heater power shifts energy input from the higher efficiency heat pump to the lower efficiency electric resistance heater, resulting in lower EF. The final RMC of the load also strongly impacts the EF, which is overlaid in Figure 3.11 with labels on the individual points.

Table 3.3. Energy breakdown for the HyHPCD tests including average measured heater and compressor power, total energy consumed, and breakdown of energy use between heaters, compressor, and motor, as well as cool-down period at the end-of-cycle with only drum motor running

Test	Type	Heater power (Watts)	Compressor power (Watts)	Total energy (kWh)	Heater energy	Compressor energy	Motor energy	Cool-down (min)
1	EXPRESS	1046	1019	1.56	36%	48%	16%	8.6
2	ECO	1041	950	1.31	7%	70%	24%	7.6
3	EXPRESS	569	986	1.42	24%	55%	21%	14.8
4	ECO	1055	952	1.39	7%	70%	23%	7.3
5	EXPRESS	715	1010	1.57	33%	50%	16%	7.6
6	ECO	1040	938	1.44	7%	69%	23%	8.0
7	ECO	1040	945	1.40	5%	70%	24%	8.2
8	EXPRESS	719	1005	1.74	27%	55%	17%	7.9
9	ECO	1034	943	1.37	9%	69%	23%	7.6
10	EXPRESS	708	1032	1.46	32%	52%	16%	7.7
11	ECO	711	999	1.23	4%	73%	23%	8.0
12	EXPRESS	493	1002	1.46	25%	56%	19%	7.2
13	ECO	713	954	1.27	5%	71%	24%	8.0
14	EXPRESS	496	992	1.50	33%	51%	16%	7.4
15	ECO	892	1042	1.53	36%	49%	15%	7.9

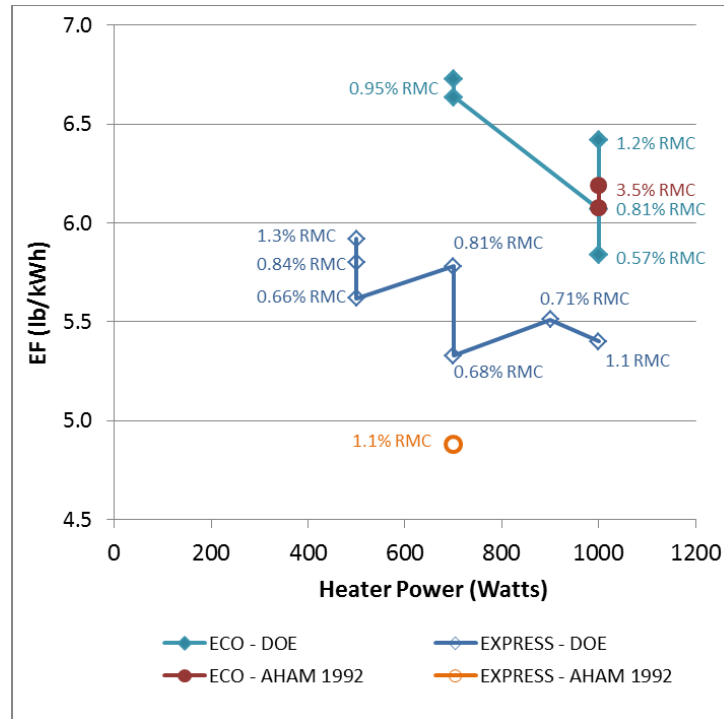


Figure 3.11. Effects of heat power and final RMC of the load on EF for the two test modes, ECO and EXPRESS, and two test loads, the standard DOE and AHAM 1992 loads

Temperatures of the refrigerant in the heat pump circuit are shown in Figure 3.12; these were obtained from thermocouples in contact with the outer surface of the piping. The condenser inlet temperature has significant superheat as expected, which allows the drying air to be heated above 80°C, as shown in Figure 3.12. As explained in Section 2.0, an important aspect of the design for obtaining high energy savings is heating the drying air as high as possible with the heat pump to minimize the amount of lower efficiency heating with the electric heaters. This was successfully accomplished with the HyHPCD, indicating the condenser was operating as designed. In addition, the temperature of the condenser outlet indicates significant subcooling, which is also important for high efficiency. However, the tracking of the evaporator inlet and outlet temperatures in Figure 3.12 indicates no superheat in the evaporator outlet, which means the TXV is not operating as intended and needs to be adjusted or replaced. A lack of superheat in the compressor suction does not hurt efficiency, but receiving liquid is hazardous for the compressor.

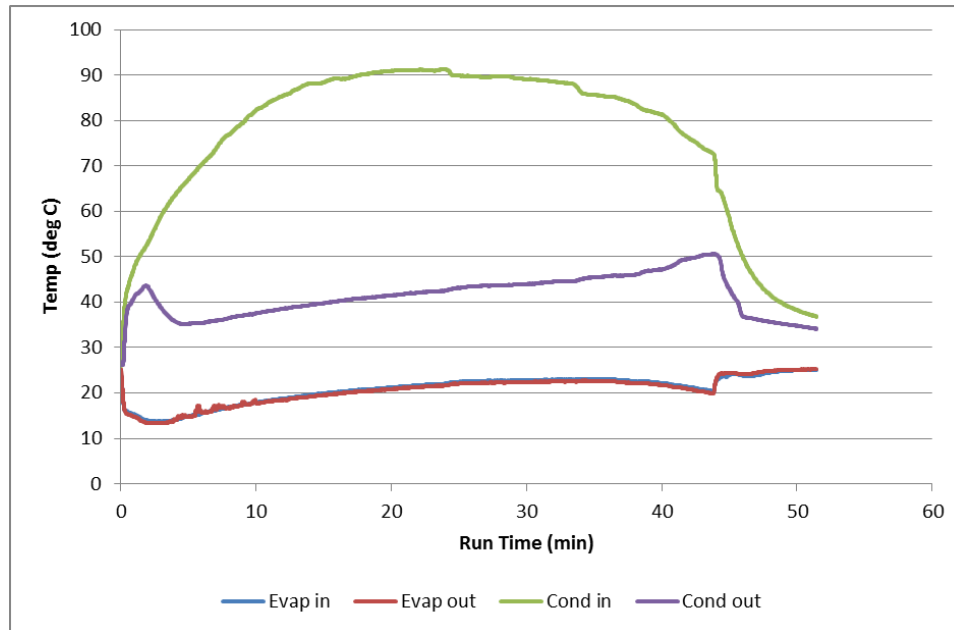


Figure 3.12. Refrigerant piping temperatures through the cycle for Test 10

3.4 Evaluation of Demonstrator Performance

Although the desired energy savings were achieved, the HyHPCD demonstrator did not perform as well as expected for initial testing of the unit as assembled. Most notably, drying times were over twice as long as expected, implying that either less energy was supplied to the load or the drying process inside the drum was less efficient. This section discusses possible causes of lower than expected performance and opportunities for improving the demonstration system. Most of the issues identified can be readily rectified through relatively simple modifications to the prototype and additional testing. The most challenging issue is pressure drops through the recuperator, which requires identifying or developing an alternative component.

The drying process could have been impacted by the modifications made inside the cabinet to direct the air flow from the condenser through the bottom of the dryer, past the electric heaters, and into the back of the drum. Although efforts were made to minimize the contact between the new baffling and the rotating drum, additional friction may have slowed the drum speed. The new flow configuration required the air to flow around the drum and past the upper half of the electric element. An altered flow distribution past the electric element and into the drum may have impacted the effectiveness of the drying process inside the drum. Evidence for a less effective drying process is the lower RH in the drum exhaust. In previous testing of the original electric dryer, the drum exhaust RH was nearly 100% during the entire CRDP in three replicate tests with the DOE test load. As indicated in Figure 3.9, the drum exhaust typically peaked at 80–90% RH and then steadily decreased to around 70% by the end of the CRDP. The lower drum exhaust RH could indicate the HyHPCD was less effective at converting sensible heat in the air to latent heat in drying the load.

Another explanation for the lower RH is air leakage. The drum exhaust RH probe was located in the flexible duct between the dryer blower exhaust and the connection to the evaporator plenum. Therefore, leakage that would affect the drum exhaust RH would have to occur upstream into the drum, most likely around door. The dryer blower pulls air through the drum which causes a slight vacuum inside the drum. Adding the pressure drop of the condenser and recuperator upstream of the drum causes the pressure in the drum to be even lower, leading to higher leakage around the door and other openings into the drum

that bypass the heaters and the load. Mixing leaked air with the drying air lowers the RH of the drum exhaust.

The possibility of air leakage can be assessed from an energy balance of the recuperative heat exchanger. Thermocouples placed in the plenums measured the temperatures of the inlet and outlet air of both the incoming cold air stream and the hot drum exhaust stream. In addition, the chamber and drum exhaust RH probes measured the moisture content of both incoming streams, respectively. All of the heat added to the incoming cold air stream goes to sensible heat, so the change in enthalpy is calculated from the temperature change. However, the hot moist drum exhaust can cool below the saturation temperature causing condensation, and the latent duty appears in the heat balance equation. The air is not at a uniform temperature in the cross-flow heat exchanger, so the air in the outlet plenum may not be saturated. Nevertheless, this is assumed in order to obtain a condensation rate from a water balance calculation that is used to obtain an estimate of the latent duty in the hot stream. The combination of the latent heat of condensation and the enthalpy change of the air stream gives the heat duty of the hot stream. Figure 3.13 shows the ratio of the cold stream duty to the hot stream duty assuming no air leakage. When the streams entering the heat exchanger are changing temperature, part of the heat duty is going to the thermal mass of the heat exchanger, which causes the heat duty ratio to change during the warm-up phase at the beginning of the cycle. At the end of the CRDP when the RH of the drum exhaust decreases, water condensate held up in the heat exchanger will evaporate and the dry out process draws more heat from the hot air and increases the heat duty ratio. The best indication of an air flow imbalance is during the CRDP when temperatures and RH of the streams are relatively constant, so the temperature of the heat exchanger mass and the water hold-up are not changing. During this period, the ratio of duties should be 1.0 if there is no air leakage. However, the duty ratio is around 0.5 during the CRDP.

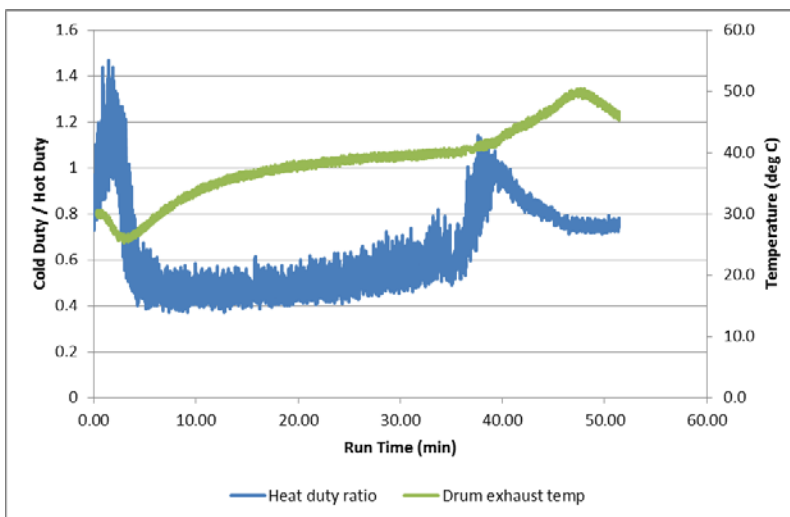


Figure 3.13. Calculated ratio of cold stream to hot stream heat duties in the recuperator assuming equal air flow on both sides

With air leaking into the drum, the air content of the drum exhaust would be higher than the air entering the drum, which causes the air flow through the hot side of the recuperator to be higher than the cold side. Correcting for higher hot stream flow would decrease the heat duty ratio further, so this does not explain the low heat duty ratio observed in Figure 3.13.

A possible explanation for the low heat duty ratio is leakage from the cold stream directly to the hot stream bypassing the dryer. This would dilute the drum exhaust stream entering the recuperator, thereby reducing the condensation rate. A lower latent duty in the hot stream would increase the duty ratio. Of course, the latent duty would be lower than calculated if the hot stream was not saturated coming out of

the recuperator. The lower latent duty only partially explains the discrepancy, however, because the ratio is still below 1.0 at the end of the cycle when condensation is not occurring in the recuperator. The ratio at the end of the cycle (~0.8) is higher than during the CRDP (~0.5), which is consistent with air leakage from the cold stream to the hot stream, so the recuperator heat balance analysis supports the possibility of air bypassing the drum.

Long drying times are also explained by less energy being supplied to the drum, which occurs if the temperature or flow rate of air entering the drum were lower than designed. The intent was for the air flow rate to be 119 CFM and for the air to be heated with 5.1 kW of energy, which would increase the temperature of 23.9°C (75°F) and 50% RH air to 97.7°C (208°F). The design called for 1.8 kW of power from an electric heater and about 2 kW of heating from the heat pump, with the balance being supplied by the recuperator during the CRDP. The heating elements could not be supplied with more than 1 kW without overheating the compressor, most likely due to insufficient cooling capacity in the condenser. This would occur if there was insufficient air flow through the condenser and into the dryer.

Air flow through the drum is estimated from a water balance of the cycle. The molar rate of water removal from the drum is

$$\dot{n}_w = \frac{\dot{V}_{ex} P}{RT_{ex}} \frac{(y_{ex} - y_{in})}{(1 - y_{in})} \quad (3.1)$$

where y_{in} and y_{ex} are the mole fraction of water in the inlet air and drum exhaust, respectively, \dot{V}_{ex} is the volumetric flow of drum exhaust assumed to be constant, P is exhaust pressure (assumed to be 1 atm), and T_{ex} is the drum exhaust temperature. The total water removed during the cycle is known from the difference in load mass between the start and end-of-cycle. The exhaust volumetric flow rate is obtained from the total water removed and the integral of Equation 3.1 over the cycle. For Test 10, the calculated drum exhaust flow rate is 92 cfm, which is 23% lower than the design value of 119 cfm obtained from the original dryer, as described in Section 2.0. This substantially lower air flow contributes to the longer drying time and the inability to run the heaters at design power.

The results of the above analyses support the supposition of insufficient air flow through the drum caused by air leakage into the drum around the door or elsewhere and/or by air bypassing the drum. As already mentioned, the lower pressure (higher vacuum) inside the drum can cause the former. Figure 3.5 shows the assembly of the heat pump heat exchangers with the plenums on the recuperator open on top. These openings were covered by a piece of foam that was compressed by the dryer on top to form seals. If this sealing method was inadequate, air could bypass the drum.

The heat exchanger pressure drops from the designs are shown in Table 3.4, showing a total added pressure drop of 1.4 in. H₂O not including losses associated with plenums, hoses, and other piping losses. Booster blowers are marketed for use when there is a very long duct from a clothes dryer to the outside vent. The booster blower used was advertised for 150 SCFM air flow for up to 150 ft of a 4 in. diameter round duct, which has a pressure drop of around 2 in. H₂O. Therefore, the booster blower should be sufficient for the added pressure drop of the heat pump system. Nevertheless, a second booster blower was added at the recuperator intake in order to better balance the pressure in the drum to reduce leakage and to increase air flow through the drum. As described above, the air flow through the drum was still lower than desired, further supporting the possibilities of air leakage and bypass.

Table 3.4. Design pressure drops for the heat pump heat exchangers

Cond coil	0.17	in.H ₂ O
Evaporator coil	0.06	in.H ₂ O
Recuperator hot side	0.56	in.H ₂ O
Recuperator cold side	0.63	in.H ₂ O
Total	1.42	in.H ₂ O

Table 3.4 indicates the biggest opportunity for improving the performance of the HyHPCD. The combined pressure drop of the recuperator is 84% of the pressure drop through the heat pump components. Reducing the recuperator pressure drops to levels comparable with the condenser and evaporator would cut the total pressure drop to 1/3. Not only would this significantly reduce the parasitic power of the blower, it would drastically reduce problems of leakage and bypass.

The recuperator is an air-to-air heat exchanger while the condenser and evaporator are air-to-phase-change heat exchangers with considerably higher overall heat transfer coefficients. This leads to a challenge in packaging a sufficient heat exchanger area in a compact device. The stacked-plate design is one viable technology, but alternative technologies, including concepts that provide for secondary heat transfer area through fin structures, should be considered. Such concepts are not as readily available as off-the-shelf components, and represent an opportunity for innovation and development.

4.0 Payback Analysis

Another objective of the project is for the payback of the HyHPCD design to be less than 5 years for 25% of the U.S. market. Our analysis projects that this is achievable in the long-term at a sales volume of 10,000 units per year. A bottoms-up analysis using vendor quotes for component costs results in a payback of 8.8 years or less for 25% of the heaviest users—households with the most drying cycles per year—at the average U.S. residential electricity rates. However, the 5-year payback is achievable with further development of the design and with volumes exceeding 10,000 units per year, which are expected to reduce the incremental price of a HyHPCD over an electric dryer to a level closer to the price of today's window air conditioners (~\$150 - \$200) that use similar heat pump components.

The payback depends on the increase in price of the HyHPCD over conventional electric dryers, the projected energy savings, and the assumed price of electricity. The incremental price of a HyHPCD is derived in two ways. The first is a bottoms-up estimate based on vendor quotes at a volume of 10,000 per year for the bill-of-materials and component specifications from the HyHPCD design. The increase in price derived by this method is \$530, which is considered an upper bound on cost subject to further optimization and supply chain negotiations.

A lower bound for the price increase is obtained by pricing window air conditioners having equivalent cooling capacity, which correspond to units rated at 6,000 to 8,000 BTU. Internet-based pricing yielded a \$155 Artic King 6,000 BTU 9.7 EER and a \$210 Frigidaire 8,000 BTU 9.8 EER window air conditioner. While the compressor selected for the HyHPCD corresponds to only 5,400 BTU of A/C cooling, the \$210 price for the higher capacity unit was selected the lower bound of the price increase.

Energy savings of 54% for a dryer that meets the DOE standard of 3.73 lbs/kWh with an 8.45-lb DOE test load [3] corresponds to a savings of 1.22 kWh/cycle. Meyers [4] calculated a distribution of annual cycles for residential clothes dryers from Energy Information Administration (EIA) 2009 Residential Electricity Consumption (RECS) data [10] that indicates that 25% of households exceed 400 cycles per year. Therefore, the potential annual energy savings exceeds 489 kWh/yr for 25% of the residential clothes dryers in the U.S.

Lastly, a residential electricity price is needed to complete a simple payback analysis. Electricity prices obtained for March 2015 from the EIA give a population weighted price of 9.35 ¢/kWh for Idaho, Washington, and Oregon, the three principal states containing BPA customers¹. The U.S. average residential electricity price is higher at 12.35 ¢/kWh, and the highest region in the country is the Northeast at 20.83 ¢/kWh.

Results from the payback analyses are tabulated in Table 4.1 for the 3 energy prices and the upper and lower bounds of the increase in purchase price. At the upper bound in dryer price, the paybacks all exceed 5 years, although only slightly for the northeast region. However, when the prices of HyHPCD dryers in significant volume sales evolve toward costs comparable to window air conditioners (~\$200), the payback periods will all shorten to less than 5 years, and can even approach 2 years in the Northeast.

¹ Electricity prices for March 2015 obtained from the EIA at <http://www.eia.gov/electricity/data.cfm>.

Table 4.1. Energy cost savings and payback based on upper and lower projections of \$530 and \$210 price increases for a HyHPCD over conventional standard electric dryers for the top 25% heaviest users in the U.S. market

Region	Residential electricity (¢/kWh)	Savings per year	Upper Payback (yrs)	Lower Payback (yrs)
Northwest	9.35	\$45.75	11.6	4.6
USA	12.35	\$60.43	8.8	3.5
Northeast	20.83	\$101.93	5.2	2.1

Rebates are a common tool used by utilities and other efficiency advocates to aid in the development of markets for appliances that exceed the current ECS and have a higher first cost. Table 4.2 provides the rebates that would facilitate a 5-year payback in the short-term when the price difference is at the estimated upper bound². There are potential additional benefits of the HyHPCD to electric utilities other than reduced energy use including reduced overall load (kW) compared to electric dryers and the potential for enabling demand response during times of capacity shortfall. Many utilities are exploring and/or offering time-based residential rate structures that can provide opportunities for utilities to compensate customers for demand response and for customers to reap monetary benefits from reduced demand. As documented in the 7th Northwest Conservation and Electric Power Plan³, future anticipated capacity shortages in the Pacific Northwest (BPA service territory) will be dependent upon load reduction through efficiency and demand response across all customer classes.

Table 4.2. Rebates for meeting a 5-year payback for 25% of consumers based on the upper bound marginal price of \$530 for a HyHPCD

Region	Residential electricity cost (¢/kWh)	Savings per year	Rebate to meet 5- year payback
Northwest	9.35	\$45.75	\$301
USA	12.35	\$60.43	\$228
Northeast	20.83	\$101.93	\$21

Simple payback is calculated by dividing the increased price of the HyHPCD by the projected annual energy cost savings based on current electricity prices. Alternative approaches could be used to determine payback including discounted projected future material costs and discounted projected future average electricity prices. Additionally, the discounted future marginal residential rate in 5 years can capture the value of the technology in terms of avoided future costs for utilities. More detailed analyses are recommended in the future when the technology matures to marketable products.

A bill-of-materials was generated from the HyHPCD design starting with an off-the-shelf 7.3 ft³ standard electric dryer and adding the major components of the heat pump system. Design specifications were used to obtain price quotations for the heat pump components from suppliers for single units and for quantities up to 10,000 units. Design of the HyHPCD evolved after the completion of the payback analysis, including modification of the heat exchangers, so the components are not completely consistent between the payback analysis and the demonstration system. Nevertheless, the payback analysis is not

² Vermont currently offer a \$400 rebate on Heat Pump Dryers, and Silicon Valley Power is offering \$100 rebates on Energy Star dryers, and many other utilities are offering ~\$50 for Energy Star dryers.

³ <https://www.nwccouncil.org/energy/powerplan/7/plan/>

expected to be significantly impacted within the margin of error. All of the components are considered off-the-shelf, although the heat exchangers are custom components of standard construction. Alternative technology is recommended for the recuperative heat exchanger that may change the cost. The list of components and their costs are provided in Table 4.3. Manufacturing labor costs of \$225 were added to the total component costs and a multiplier of 1.3 was applied for markup to arrive at an estimated consumer retail price of \$1,279.

Table 4.3. Major component costs based vendor quotes for the HyHPCD

Component	Manufacturer	Model	OTS?	Price ea., Quantity 1	Price ea., Quantity 10,000
Compressor	Embraco	FFI12HBX	Y	\$ 250.42	\$ 79.42
Expansion Valve	Parker Hannafin (Sporland Division)	EFJ1C	Y	\$ 85.73	\$ 50.00
Evaporator	Super Radiator	Per Drawing	Y	\$ 531.00	\$ 88.00
Condenser	Super Radiator	Per Drawing	Y	\$ 711.00	\$ 166.00
Recuperator	HeatEX	HA0200-0177-016- 4AOO-2-0-0-0177	Y	\$ 62.00	\$ 54.00
7.3 ft ³ Electric Dryer	Open Source	Open Source	Y	\$ 402.00	\$ 321.60
Total				\$ 2,042.15	\$759.02

In order to compute an incremental price, the HyHPCD estimate price was compared to the LG Model DLE1101W, a mid-range standard 7.3-cubic-foot electric clothes dryer, priced at \$749. This gives an estimated price difference of \$530 between the HyHPCD and conventional standard electric dryers. This can be considered an upper bound, since the design has not been optimized for cost and component costs are expected to decrease with further negotiations with suppliers.

Window air conditioners have similar components to the heat pump system being integrated into the HyHPCD and, as mature commercial products, can provide a lower bound for the cost of HyHPCD equipment. For example, the Embraco compressor is rated for 5,364 Btu/hr cooling capacity at condensing and evaporating temperatures of 40.6°C (105°F) and 7.2°C (45°F), respectively, which is compatible with the conditions used for rating air conditioners.

However, there are differences between the HyHPCD heat pump system and window air conditioners. Components in a window A/C unit that are not needed in the HyHPCD include the air mover—two fans and a motor—and the controls, which are redundant with components already in the clothes dryer. On the other hand, the HyHPCD includes an extra recuperative heat exchanger and a unique condenser design, which are not part of window A/C units. The operating temperatures are very different, so the other heat exchangers are not directly transferable. Therefore, prices of window air conditioners at similar cooling capacities required for a HyPCD are only an indication of potential cost reductions in the HyHPCD equipment, but this is the best option for setting a lower bound on the price increase.

Internet pricing for 6,000-8,000 BTU window air conditioners yields a considerable range, but included an Artic King 6,000 BTU for \$155 and a Frigidaire 8,000 BTU for \$210 in March 2015. The compressors in these units are rated at higher cooling capacity than the Embraco compressor selected for the HyHPCD. It is highly likely that the compressors in these units cost the manufacturers less than \$79 given the retail price and understanding of typical appliance markup. This is evidence that there is potential for cost reductions in the HyHPCD below the estimate derived from vendor quotes.

The uncertainty in the payback analysis is addressed by bounding the projected price increase of the HyHPCD over conventional electric dryers. The upper bound is taken from the bottoms-up cost estimate derived from the bill-of-materials. The higher price of \$210 for the Frigidaire 8,000 BTU window air conditioner is adopted for the lower bound. The final price reached through design optimization and product development is expected to fall within these bounds, which includes the potential for reaching a 5-year payback for at least 25% of the U.S. and Northwest residential clothes dryer markets.

5.0 Conclusions and Recommendations

Through modeling and an experimental prototype, the potential for ‘moving the bar’ in reducing energy consumption of residential clothes dryers has been demonstrated with affordable, off-the-shelf heat pump technology. The prototype design promises energy savings of greater than 50% with comparable drying times of around 40 minutes when adding a heat pump system to commercial electric clothes dryers. This is based on detailed modeling supported with test data from a standard vented electric dryer. The experimental prototype exceeded 50% energy savings, but with drying times of over an hour. This achievement represents a step change in energy savings over the three standard heat pump clothes dryers currently offered in the U.S. market.

A bottoms-up analysis of the cost of components concluded a payback of 9 and 12 years for the northwest and the overall U.S., respectively, for 25% of the residential market. These paybacks are expected to decrease to less than 5 years with design refinement and further supply chain negotiations. This represents affordability to a significant fraction of the U.S. residential market, which can be greatly expanded with utility rebate or other incentive programs.

The gap between design and performance of the experimental prototype is attributed to less energy being supplied to the load in drum as well as impacts on the drying process due to the modifications. Test results indicate potential leakage of air into the drum bypassing the heaters as well as air bypassing the drum, leading to lower drying rates and longer drying times. These problems can be easily addressed through further development of the prototype.

A more challenging issue is the pressure drop through the recuperative heat exchanger, an important component contributing to energy savings. The stacked-plate heat exchanger used for the recuperator in the prototype is the largest component and accounts for 84% of the pressure drop. Alternative technology for compact air-to-air heat exchange with lower pressure drops is needed, but fewer off-the-shelf options are available. Advancing heat exchanger technology for this specific application represents the most significant opportunity for development and the movement of the technology into the market.

For convenience, this project started with a commercial standard-size vented electric dryer, and modifications were made to seal the cabinet and redirect the flow path through the dryer. While this approach was successful and demonstrated the desired energy savings, the system is not considered a prototype. Sealing the dryer cabinet prevented the drum motor from receiving adequate cooling causing it to run considerably hotter than the nameplate temperature. A booster blower was added to compensate for the pressure drop of the heat pump components. A better solution is to replace the existing drum blower and motor with components capable of providing full air flow at the overall system pressure drop. A next step is to develop a true prototype that eliminates these shortcuts, packages the heat pump system into a pedestal under the dryer, and resolves the issues identified above. Additional development of the control system is needed to optimize energy savings and to add auto termination. These future developments are intended to be accomplished with the help of OEM expertise.

6.0 References

1. TeGrotenhuis, WE. 2014. "Clothes Dryer Automatic Termination Sensor Evaluation: Volume 1: Characterization of Energy Use in Residential Clothes Dryers". PNNL-23621. Pacific Northwest National Laboratory, Richland, WA.
2. 78(1) FR 152-185. January 2, 2013. "Energy Conservation Program: Test Procedures for Residential Clothes Dryers" U.S. Department of Energy, Federal Register.
3. 78(157) FR 49608-49651. August 14, 2013. "Energy Conservation Program: Test Procedures for Residential Clothes Dryers" U.S. Department of Energy, Federal Register.
4. Meyers, S., V. Franco, A. Lekov, L. Thompson, and A. Sturgen. 2010. "Do Heat Pump Clothes Dryers Make Sense for the U.S. Market?, in 2010 ACEEE Summer Study of Energy Efficiency in Buildings". Lawrence Berkeley National Laboratory, Berkeley, CA.
5. Brendt, P., C. Calwell, and L. Morefield. 2009. "Residential Clothes Dryers: An Investigation of Energy Efficiency Test Procedures and Savings Opportunities". 2009, Ecos report for the Natural Resources Defense Council, November 6, 2009.
6. Pescatore, P. and P. Carbone. 2005. "High Efficiency, High Performance Clothes Dryer". TIAX Final Report to: Department of Energy, Reporting Period 9-30-01—3/31/03, March 31, 2005. TIAX LLC, Cambridge, MA.
7. Ng, A.B. and S. Deng. 2008. "A new termination control method for a clothes drying process in a clothes dryer". Applied Energy, 2008. **85**(9): p. 818-829.
8. American National Standards Institute (ANSI)/ American National Standards Institute (AHRI). 2004. "Standard For Performance Rating Of Positive Displacement Refrigerant Compressors And Compressor Units". ANSI/AHRI Standard 540-2004.
9. Association of Home Appliance Manufacturers (AHAM) HLD-1-1992. 1992. "Household Tumble Type Clothes Dryers." Association of Home Appliance Manufacturers, Washington, DC.
10. Energy Information Administration (EIA). 2012a. "Estimated U.S. Residential Electricity Consumption by End-Use, 2010." U.S. Department of Energy.

Appendix A

The information in Appendix A includes pictures, equipment specifications, and drawings for the heat pump components, including the condenser, evaporator, recuperative heat exchanger, compressor, and TXV. Pictures of the front view and side view of the condenser are shown in Figure A.1, with a coffee cup included for perspective. The condenser is oriented horizontally on the front side of the heat pump assembly shown in Figure 3.5. The evaporator is shown in Figure A.2. Both the condenser and evaporator were designed and made by Super Radiator Coils from specifications provided. The two stacked-plate recuperative heat exchangers obtained from HeatEx are shown in Figure A.3, and the smaller one was used in the demonstration system. The Embraco Model FFI12HBX-EJ compressor is shown in Figure A.4 while in the process of being installed in the heat pump system. The condenser and evaporator components were designed to the specifications in Figures A.5 to A.7. The condenser components was split between the condenser specifications in Figure A.5 and the subcooler specifications in Figure A.6. The design specifications for the recuperator from HeatEx are given in Figure A.8. Table A.1 shows the correlations that were provided for the Embraco Model FFI12HBX-EJ compressor for predicting cooling capacity, power consumption, efficiency, current, and mass flow as functions of the evaporation and condensation temperatures. The correlations were developed from a condensing temperature range of 35°C to 65°C and an evaporating temperature range of -35°C to 15°C. The correlations were extrapolated up to 70°C in the design calculations. Lastly, drawings of the evaporator and condenser coils are shown in Figures A.9 and A.10.



Figure A.1. Front and side views of the condenser component designed and made to specifications by Super Radiator Coils; coffee cup is included for perspective.



Figure A.2. Front view of the evaporator component designed and made to specifications by Super Radiator Coils.



Figure A.3. Two recuperative heat exchangers of different size obtained from HeatEx; the smaller heat exchanger was used in the heat pump system.



Figure A.4. Embraco Model FFI12HBX-EJ compressor shown being installed in the heat pump system.



		SUPER RADIATOR COILS.		Version: 3.2.0.0 P-2015
Customer:				Date: 9/1/2015
Project: Jabil				By: Jian Yu
Item: deSuperHeat/Condenser				Units: English
Condenser Coil	Coil Qty: 1	Model: 6x10 - 8R - 0.197/180		
Input				
Airside Requirements:				
Surface Condition:		Dry		
Air Flow:	Lbs./hr. Dry Air	489		
Capacity:	Btu/Hr.	7513		
Entering Air Dry-Bulb:	°F	110		
Leaving Air Dry-Bulb:	°F	173.1		
Air Pressure:	PSIA	14.696		
Coil Hand:		Vert up Airflow		
Tubeside Requirements:				
Refrigerant:		R-134a		
Condensing Temp.:	°F	158		
Hot Gas Temp.:	°F	238.5		
Subcooling Degrees:	°F	0.5		
Output				
Coil Selection:				
Model Number:		6x10 - 8R - 0.197/180		
Tube Size:	In.	0.197		
Arrangement:		0.75 x 0.449 Staggered		
Fin Surface:		Raised Lanced		
Face Area / Coil:	ft²	0.4		
Face Velocity / Coil:	Ft/Min. (STD)	260.8		
Number Of Circuits:	Qty	4		
Circuitry Flow:		Thermal Counter Flow		
Tube Material:		Copper		
Tube Wall:	In.	0.010R		
Fin Material:		Aluminum		
Fin Thickness:	In.	0.0039		
Header OD (HG/Liq):	In.	0.375 / 0.375		
Header Material:		Std.Type 'L' Copper		
Connection OD:	In.	0.375 / 0.375		
Casing Material:		16 Ga. Galv. Steel (Std.)		
Casing Depth:	In.	4		
Weight:	Lbs./Coil	10		
Coil Rating				
Capacity:				
Capacity / Coil:	Btu/Hr.	7516		
Leaving Air Dry-Bulb:	°F	173		
Air Friction:	In.H ₂ O/Coil	0.25		
Surface Condition:		Dry		
Subcooling Degrees:	°F	0.5		
Refrig. Press. Drop:	PSI/Coil	3.5		
Refrig. Mass Flow:	Lbs./Hr.	95		
Super Radiator Coils - www.SuperRadiatorCoils.com 451 Southlake Blvd. Richmond, VA 23236-3091 - (800) 229-2645				

Figure A.5. Final specifications for the condenser component from Super Radiator Coils.

 SUPER RADIATOR COILS.		Version: 1.2.0.0 4/2015
Customer:		Date: 9/1/2015
Project: Jabil	By: Jian Yu	
Item: Subcooler	Units: English	
Other Fluid Coil	Coil Qty: 1	Model: 6x10 - 2R - 0.197/180
Input		
Airside Requirements:		
Coil Application:		Heating
Air Flow:	Lbs/hr. Dry Air	489
Capacity:	Btu/Hr.	1688
Entering Air Dry-Bulb:	°F	95.8
Leaving Air Dry-Bulb:	°F	110
Air Pressure:	PSIA	14.696
Coil Hand:		vert up Airflow
Tubeside Requirements:		
Tubeside Fluid:		R134a
Flow Rate:	GPM	0.181
Entering Fluid Temperature:	°F	158
Specific Heat:	Btu/(lb-F)	0.3839
Specific Gravity:		1.0743
Viscosity:	(cP)	0.0393
Thermal Conductivity:	Btu/(hr-ft-F)	0.0393
Reference Temperature:	°F	135.33
Output		
Coil Selection:		
Model Number:		6x10 - 2R - 0.197/180
Tube Size:	In.	0.197
Arrangement:		0.75 x 0.449 Staggered
Fin Surface:		Raised Lanced
Face Area / Coil:	ft²	0.4
Face Velocity / Coil:	Ft/Min. (STD)	260.8
Number Of Circuits:	Qty	1
Tube Velocity:	Ft/Second	2.04
Circuitry Flow:		Cross Flow
Tube Material:		Copper
Tube Wall:	In.	0.010R
Fin Material:		Aluminum
Fin Thickness:	In.	0.0039
Header OD:	In.	0.375
Header Material:		Std.Type 'L' Copper
Connection OD:	In.	0.375
Casing Material:		16 Ga. Galv. Steel (Std.)
Casing Depth:	In.	2
Weight:	Lbs./Coil	10
Coil Rating		
Capacity:		
Capacity / Coil:	Btu/Hr.	1690
Leaving Air Dry-Bulb:	°F	110
Air Friction:	In.H ₂ O/Coil	0.05
Surface Condition:		Dry
Leaving Fluid Temperature:	°F	112.66
Fluid Pressure Drop:	psi	1.38

Super Radiator Coils • www.SuperRadiatorCoils.com
 451 Southlake Blvd. Richmond, VA 23236-3091 • (800) 229-2645

Figure A.6. Final specifications for the subcooler component from Super Radiator Coils.


		Version: 3.1.6.0 © 2015	
Customer: Jabil Circuit, Inc.		Date: 5/8/2015	
Project: New System Design		By: Louis Rogerson	
Item: Evaporator- IP Units		Units: English	
Evaporator Coil		Coil Qty: 1	Model: 9x9 - 3R - 0.375/168
Input			
Airside Requirements:			
Coil Application:		Cooling	
Surface Condition:		Wet	
Air Flow:	SCFM	98	
Capacity:	Btu/Hr.	6,000	
Entering Air Dry-Bulb:	°F	93.1	
Entering Air Wet-Bulb:	°F	93.1	
Leaving Air Wet-Bulb:	°F	81.9	
Air Pressure:	PSIA	14.696	
Coil Hand:		Left Hand	
Tubeside Requirements:			
Refrigerant:		R-134a	
Refrigerant Suction Temp.:	°F	73.4	
Degrees Superheat:	°F	5.0	
Liquid Temperature:	°F	125.0	
Refrig. Mass Flow:	Lbs./Hr.	109	
Output			
Coil Selection:			
Model Number:		9x9 - 3R - 0.375/168	
Legacy Part Number:		11X00900090-0103EW00002-C01A02AXXNL	
Tube Size:	In.	0.375	
Arrangement:		1 x 0.866 Staggered	
Fin Surface:		X Fin	
Face Area / Coil:	ft²	0.6	
Face Velocity / Coil:	Ft/Min. (STD)	174.2	
Number Of Circuits:	Qty	1	
Circuitry Flow:		Thermal Parallel Flow	
Tube Material:		Copper	
Tube Wall:	In.	0.015R	
Fin Material:		Aluminum	
Fin Thickness:	In.	0.0055	
Casing Material:		.063 Aluminum	
Casing Depth:	In.	4.625	
Weight:	Lbs./Coil	7	
Coil Rating			
Capacity:			
Capacity / Coil:	Btu/Hr.	6,587	
Sensible Cap. / Coil:	Btu/Hr.	1,341	
Leaving Air Dry-Bulb:	°F	80.6	
Leaving Air Wet-Bulb:	°F	80.6	
Air Friction:	In.H ₂ O/Coil	0.22	
Surface Condition:		Wet	
Refrigerant Inlet Temp.:	°F	76.4	
Refrig. Press. Drop:	PSI/Coil	4.605	
Circuit Loading:	Btu/Hr.	6,587	

Figure A.7. Final specifications for the evaporator component from Super Radiator Coils.

HEATEX

HEATEX AB Sweden, www.heatex.com

5/20/2015

Version: 505.0

Customer: Jabil
Object: 7 inches



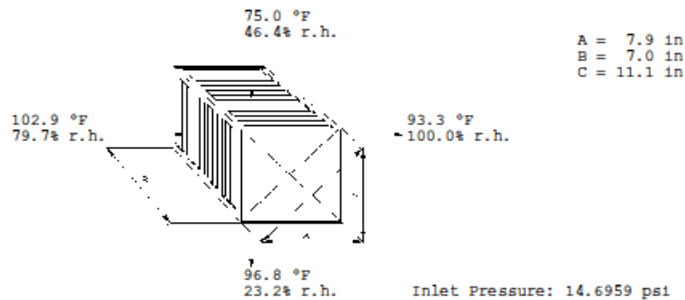
DESCRIPTION

Heat Exchanger:	H0200/1.6/A	HA0200-0177-016-4AOO-2-0-0-0177
Plates:	Aluminium with turbulence surface.	
Frames:	Flat end plate (Aluminium) 1.5 mm (0.06 in). Brush Al Profile	
Sealing:	Silicone free (max 190°F)	
Consists of:	1 Module	Nominal plate distance: .06 in
Number of steps:	1	Total Width: 7.0 in
Total Exchanger Weight:	5.7 lb	

RESULT (Summer)

	Exhaust Air	Supply Air
Air flow:	115 SCFM (.065 kg/s)	124 SCFM (.07 kg/s)
Pressure drop: *)	.56 / .54 inch H2O	.63 / .6 inch H2O
Efficiency:	34%	78%
Air Velocity: (face/channel)	304.59 / 827.43 ft/min	345.57 / 911.58 ft/min
Condensate:	1.2 lb/h, tcond 95.4 °F	
Transferred Power:	2686 BTU/h	

* (Actual pressure drop/Pressure drop corrected to density 1.2 kg/m3)



The calculations are made in accordance with the European norm EN308 and its sub documents
Owing to continued product development Heatex AB reserves the right to introduce alterations both in design and prices without prior notice.

Figure A.8. Final specifications for the recuperator component from HeatEx.

Table A.1. Correlation coefficients for the Embraco Model FFI12HBX-EJ compressor where ET and CT are the evaporation and condensation temperatures, respectively.

$A + (B * ET) + (C * CT) + (D * ET * CT) + (E * (ET)^2) + (F * (CT)^2) + (G * (ET)^2 * CT) + (H * ET * (CT)^2) + (I * (ET)^3) + (J * (CT)^3)$					
	Capacity (Btu/h)	Power (Watts)	Efficiency	Current (Amps)	Mass Flow (kg/h)
A	4.2323E+03	3.2886E+02	1.2057E+01	5.6567E+00	2.4467E+01
B	1.5147E+02	5.7844E+00	2.5133E-01	3.5113E-02	9.0620E-01
C	1.5089E+00	4.0196E+00	-1.0255E-01	1.4360E-04	9.1078E-03
D	4.9364E-01	4.1250E-02	-1.7839E-03	3.4464E-04	2.8376E-03
E	2.1093E+00	3.1840E-02	1.5681E-03	1.9668E-04	1.3757E-02
F	-1.4033E-01	-7.4762E-03	3.1005E-04	1.8690E-04	-8.1690E-04
G	2.4107E-03	7.0536E-04	-2.6536E-05	1.6518E-05	1.3196E-05
H	-4.2000E-03	1.0857E-03	1.1714E-06	7.8571E-06	-2.4857E-05
I	6.8765E-03	3.7037E-04	-1.4293E-05	3.7037E-06	6.2216E-05
J	0.0000E+00	0.0000E+00	0.0000E+00	0.0000E+00	0.0000E+00

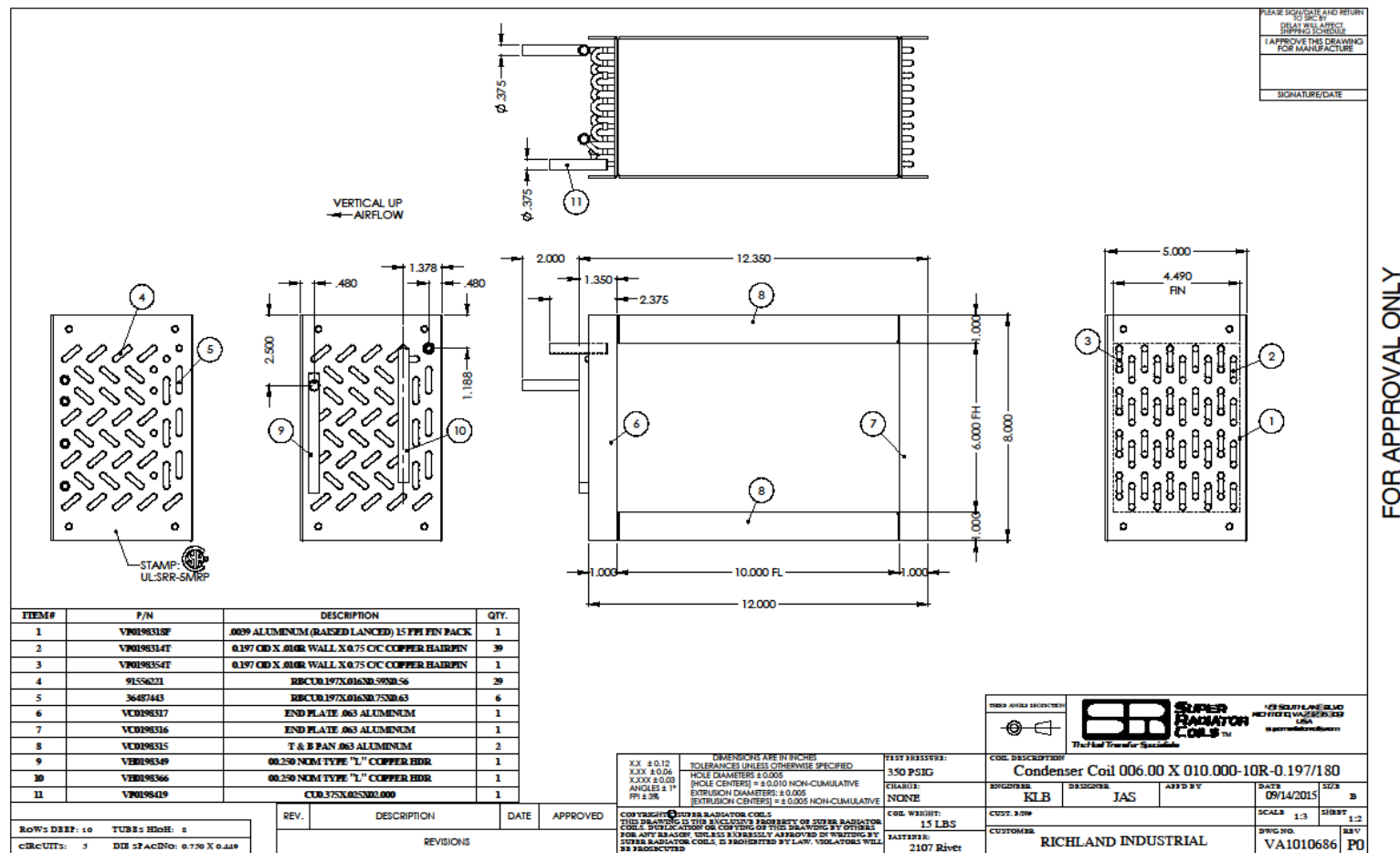


Figure A.9. Drawing of the Condenser Coil from Super Radiator Coils.



Pacific Northwest
NATIONAL LABORATORY

*Proudly Operated by **Battelle** Since 1965*

902 Battelle Boulevard
P.O. Box 999
Richland, WA 99352
1-888-375-PNNL (7665)

U.S. DEPARTMENT OF
ENERGY

www.pnnl.gov